

Sum rules of L -edge x-ray magnetic circularly polarized emission for $3d$ transition metals

Akihiro Koide, Takuji Nomura, and Toshiya Inami 

Synchrotron Radiation Research Center, National Institutes for Quantum and Radiological Science and Technology, SPring-8, 1-1-1 Koto, Sayo, Hyogo 679-5148, Japan



(Received 24 May 2021; accepted 23 August 2021; published 14 September 2021)

We propose sum rules of x-ray magnetic circularly polarized emission (XMCPE) at L edges for $3d$ transition metals. By making use of combinations of incident and emitted photon helicities, z -component expectation values of spin, orbital, magnetic dipole, and quadrupole terms can be obtained separately. The fundamental difference in the sum rules between x-ray magnetic circular dichroism and XMCPE arises from the variety of electron transitions involving core states split by the spin-orbit interaction. The additional electron transition in XMCPE causes complicated angular dependence of the sum rule relation for the spin moment. Our findings promote future L -edge XMCPE measurements, which have not been observed at present.

DOI: [10.1103/PhysRevB.104.094419](https://doi.org/10.1103/PhysRevB.104.094419)

I. INTRODUCTION

X-ray magnetic circular dichroism (XMCD) is one of the most powerful techniques to reveal local magnetic properties around the x-ray absorbing atom in various materials [1–3]. In particular, the sum rules of L -edge XMCD provide the local orbital moment and effective spin moment separately [4–10]. Although the effective spin moment comprises not only the pure spin moment but also the magnetic dipole moment, the extraction of each magnetic contribution from the total magnetic moment is unique and an advantage of XMCD.

Instead of observing XMCD, magnetic circular dichroism of the emission spectra at the L edges has been used, where the incident circular polarization is flipped [11–22]. Whereas the absorption spectroscopies including XMCD reflect properties in the unoccupied states basically, it was expected that magnetic properties in the occupied states are obtained more directly by this emission technique than by XMCD. However, to our knowledge, no sum rule of the x-ray emission has been proposed, and thus XMCD has been still the unique x-ray spectroscopic technique to provide quantitative information.

Recently, Inami has developed a novel x-ray emission spectroscopy, called x-ray magnetic circularly polarized emission (XMCPE), which detects circularly polarized x rays emitted from a magnetized sample [23]. XMCPE has been confirmed for metallic iron in the $K\alpha$ emission [23]. In the $K\alpha$ emission, first a $1s$ electron is excited to a photoelectron state by an incident x-ray photon, and subsequently x rays are emitted by electron transition from $2p$ to $1s$ states. Because the $1s$ hole has no orbital moment and the photoelectron energy does not depend on the orbital moment, the polarization of the incident x rays has no effect on K -edge XMCPE. On the other hand, the energy levels of the $2p$ states are split by the interaction with the spin-polarized $3d$ states in $3d$ transition metal (TM) magnets, which provides magnetic circular

dichroism of K -edge XMCPE. Detailed shapes of the K -edge XMCPE spectra have been investigated theoretically by using a Keldysh Green's function approach, which elucidates the contribution of the continuum nature of the $3d$ band structures in metallic iron [24]. Although $3d$ electron excitation due to a many-body effect contributes to K -edge XMCPE spectra in TMs, the existence of sum rules based on the $3d \rightarrow 3d$ indirect electron transition cannot be guaranteed. On the other hand, L -edge XMCPE where $3d \rightarrow 2p$ direct transition is dominant in itinerant TMs has a potential to provide new sum rules by making use of the polarization of the incident and emission x rays. Although L -edge XMCPE for TMs has not been observed at present, such new sum rules are closely related to the occupied $3d$ states and could make x-ray emission spectroscopy more quantitative and useful in the future.

This paper presents sum rules of L -edge XMCPE for $3d$ TMs and is organized as follows. In Sec. II A, the Hamiltonian that describes our system is given. In Sec. II B, the transition probability from incident to outgoing photons is calculated by a Keldysh diagram and Keldysh Green's functions. The integration of L -edge XMCPE spectra converts the $3d$ Green's functions to the $3d$ -electron-number matrices, which play an essential role in the derivation of the sum rule relations. In Sec. II C, we show sum rules providing z components of magnetic dipole, quadrupole, and spin terms (T_z , Q_{zz} , and S_z). In Sec. III, the dependence of the sum rule relations on the incident and emitted x-ray angles is exhibited. In Sec. IV, the origin of the angular dependence and the difference between XMCPE and XMCD are discussed. We also comment on practical measurements of L -edge XMCPE. Section V provides the conclusion. An example of calculated XMCPE spectra within the Hartree-Fock approximation is shown in Appendix A. Details of the dipole transition matrices are explained in Appendix B. The representation of characteristic functions which is used to derive sum rules is discussed in Appendix C.

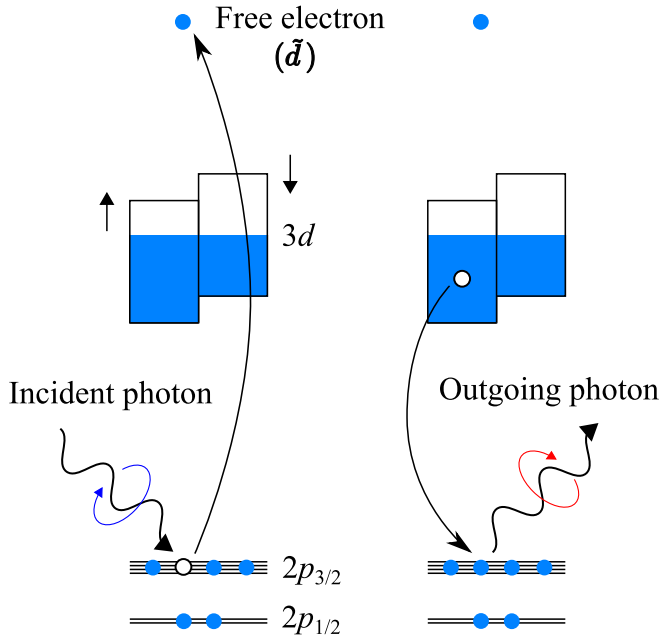


FIG. 1. Schematic of a typical $L\alpha$ XMCPE process. (Left) A $2p_{3/2}$ electron is excited to a photoelectron state by an incident x-ray photon in the first step of $L\alpha$ XMCPE. The photoelectron state is approximated to a free electron state denoted by \vec{d} . The $2p$ hole state depends on the polarization and angle of the incident photon. (Right) A circularly polarized photon is emitted by the relaxation of a $3d$ electron to the $2p$ state. The circular polarization originates from the angular momentum conservation in the $2p$ hole annihilation and the $3d$ hole creation. The relative positions among the electron energy levels are depicted schematically and not quantitatively precise.

II. THEORETICAL FORMULATION

The basic physical concept of L -edge XMCPE described here is similar to that of K -edge XMCPE shown in Ref. [24]. A schematic picture of an $L\alpha$ XMCPE process, where a $2p_{3/2}$ hole is buried by a $3d$ electron, is depicted in Fig. 1. The $L\beta$ emission corresponding to the relaxation of a $2p_{1/2}$ hole can be described by the same manner as the $L\alpha$ emission. It is assumed that, in the XMCPE measurements, the incident x-ray energy is fixed and the emitted x-ray energy is scanned. Substantial difference between K - and L -edge XMCPE is the degrees of freedom in the intermediate (or first) hole states. A $1s$ hole state only has the spin degrees of freedom and is not influenced by the spin-orbit coupling, which leads to no dependence on the incident polarization and angle in K -edge XMCPE. Meanwhile, a $2p$ hole state has the spin and orbital degrees of freedom and they are coupled by the spin-orbit interaction, which causes the incident polarization dependence and the incident angular dependence, in L -edge XMCPE. In this paper all the equations are given in the Hartree atomic units and all the values of the spin indices are a half integer.

We adopt a Keldysh Green's function approach, which was also used to investigate K -edge XMCPE spectra of metallic iron [24]. There are two main advantages of the approach. The one is that L -edge XMCPE theory can be compared to the K -edge one easily. The other is that the L -edge XMCPE sum rules should be derived as generally as possible in order

to make their limitation clear because there is no experimental data to compare with theoretical results. We shall see that the local $3d$ electron number appears for any choice of $3d$ Hamiltonian with small $3d$ spin-orbit interaction, which enables us to derive the XMCPE sum rules.

A. Hamiltonian

The total Hamiltonian H consists of the unperturbed Hamiltonian H_0 and the electron-photon interaction H_x :

$$H = H_0 + H_x. \quad (1)$$

H_0 consists of the electron and radiation-field parts:

$$H_0 = H_e + h_r. \quad (2)$$

Before explaining the electron Hamiltonian H_e , we describe H_x and the radiation-field Hamiltonian h_r . h_r is given by

$$h_r = \sum_{\Lambda} \varepsilon_{\Lambda} a_{\Lambda}^{\dagger} a_{\Lambda} \quad [\Lambda \equiv (\mathbf{k}_r, \lambda)], \quad (3)$$

where \mathbf{k}_r and λ are the momentum vector and polarization of a photon, respectively. For simplicity, we label a photon with the index Λ . a_{Λ}^{\dagger} and a_{Λ} are the creation and annihilation operators of the photon labeled with Λ , respectively, and ε_{Λ} is the photon energy.

H_x is expressed by the momentum operator \mathbf{p} and the vector potential \mathbf{A} in the Coulomb gauge:

$$\begin{aligned} H_x &= \sum_{\alpha, \alpha'} \langle \psi_{\alpha} | \left(-\frac{1}{c} \right) (\mathbf{A} \cdot \mathbf{p}) | \psi_{\alpha'} \rangle c_{\alpha}^{\dagger} c_{\alpha'} \\ &= \sum_{\alpha, \alpha'} \sum_{\Lambda} w_{\alpha\alpha'}(\Lambda) c_{\alpha}^{\dagger} c_{\alpha'} a_{\Lambda} + (\text{H.c.}), \end{aligned} \quad (4)$$

where c is the speed of light and its value is about 137 in the Hartree atomic units. The indices α and α' specify each state of the $2p$ or $3d$ electrons or the photoelectron forming a basis of H_e , which is explained below. ψ_{α} is the electron wave function of the α state. c_{α}^{\dagger} (c_{α}) is the creation (annihilation) operator of the α electron. We apply the dipole approximation to the matrix element w :

$$w_{\alpha\alpha'}(\Lambda) \propto \frac{1}{\sqrt{\varepsilon_{\Lambda}}} \langle \psi_{\alpha} | (\hat{\varepsilon}_{\lambda} \cdot \mathbf{p}) | \psi_{\alpha'} \rangle, \quad (5)$$

where $\hat{\varepsilon}_{\lambda}$ is the polarization vector with the λ polarization.

H_e consists of the terms for the $2p$, photoelectron, and band states, and the $2p$ - $3d$ interaction:

$$H_e = h_{\vec{d}} + h_{2p} + H_{\text{band}} + V_{pd}. \quad (6)$$

The photoelectron Hamiltonian $h_{\vec{d}}$ is assumed to be

$$h_{\vec{d}} = \sum_{\mathbf{k}, \mathbf{G}} \sum_{\sigma} \varepsilon_{|\mathbf{k}+\mathbf{G}|} c_{\mathbf{k}, \mathbf{G}, \sigma}^{\dagger} c_{\mathbf{k}, \mathbf{G}, \sigma} \equiv \sum_{\mathbf{K}} \sum_{\sigma} \varepsilon_{\mathbf{K}} c_{\mathbf{K}, \sigma}^{\dagger} c_{\mathbf{K}, \sigma}, \quad (7)$$

where \mathbf{k} , \mathbf{G} , and i indicate a crystal-momentum vector in the first Brillouin zone, a reciprocal lattice vector, and a unit cell, respectively. The index σ shows the up ($\uparrow = +1/2$) or down ($\downarrow = -1/2$) spin. $c_{\mathbf{K}, \sigma}^{\dagger}$ and $c_{\mathbf{K}, \sigma}$ are the creation and annihilation operators of the photoelectron with the momentum vector \mathbf{K} in the extended zone scheme and the spin σ . We assume that the photoelectron energy $\varepsilon_{\mathbf{K}}$ is sufficiently large to consider

the photoelectron as a free electron, whose energy does not depend on σ .

The $2p$ Hamiltonian h_{2p} includes the spin-orbit interaction:

$$h_{2p} = \sum_{\mathbf{k}} \sum_{\zeta, \zeta'} [\varepsilon_{2p} \delta_{\zeta \zeta'} + \varepsilon_{2p}^{\text{soc}} (\mathbf{l} \cdot \mathbf{s})_{\zeta \zeta'}] c_{\mathbf{k}, \zeta}^\dagger c_{\mathbf{k}, \zeta'}, \quad (8)$$

where the indices ζ and ζ' indicate the magnetic quantum number and the spin index to specify each $2p$ state. $c_{\mathbf{k}, \zeta}^\dagger$ and $c_{\mathbf{k}, \zeta}$ are the creation and annihilation operators of the $2p$ electron with \mathbf{k} and ζ , respectively. The bare $2p$ energy ε_{2p} does not depend on \mathbf{k} . The spin-orbit interaction is described by the orbital angular momentum vector \mathbf{l} , the spin vector \mathbf{s} , and the coupling energy $\varepsilon_{2p}^{\text{soc}}$.

The band Hamiltonian H_{band} including $3d$ states dominates the values of the physical quantities and detailed shapes of L -edge XMCPE spectra (see Appendix A). However, the explicit form of H_{band} does not appear because the expectation value of the $3d$ electron number is only used for deriving the sum rules.

The $2p$ - $3d$ interaction V_{pd} is given by

$$V_{pd} = \frac{1}{N} \sum_{\mathbf{k}, \mathbf{k}', \mathbf{q}} \sum_{\zeta, \zeta'} \sum_{\xi, \xi'} v_{\zeta \zeta', \xi \xi'} c_{\mathbf{k}, \zeta}^\dagger c_{\mathbf{k}', \xi}^\dagger c_{\mathbf{k}'+\mathbf{q}, \xi} c_{\mathbf{k}-\mathbf{q}, \zeta'}, \quad (9)$$

where the index ξ indicates each $3d$ state specified by the magnetic quantum number and the spin index. $c_{\mathbf{k}, \xi}^\dagger$ and $c_{\mathbf{k}, \xi}$ are the creation and annihilation operators of the $3d$ electron specified by \mathbf{k} and ξ , respectively. The momentum \mathbf{q} is transferred between the $2p$ and $3d$ states. N is the number of \mathbf{k} points in the first Brillouin zone. We assume that the $2p$ states preserve the nature of the eigenstates for the total angular momentum and its z component due to the strong spin-orbit interaction. This assumption can be expressed by use of the mean-field $2p$ Hamiltonian \bar{H}_{2p} defined as follows:

$$\bar{V}_{pd} \equiv \sum_{\mathbf{k}} \sum_{\zeta, \zeta'} \sum_{\xi, \xi'} v_{\zeta \zeta', \xi \xi'} n_{\xi, \xi'}^{3d} c_{\mathbf{k}, \zeta}^\dagger c_{\mathbf{k}, \zeta'}, \quad (10)$$

$$n_{\xi, \xi'}^{3d} = \frac{1}{N} \sum_{\mathbf{k}'} \langle c_{\mathbf{k}', \xi}^\dagger c_{\mathbf{k}', \xi'} \rangle, \quad (11)$$

$$\bar{H}_{2p} \equiv h_{2p} + \bar{V}_{pd} = \sum_{j, \mu} \varepsilon_{j, \mu} c_{\mathbf{k}, j, \mu}^\dagger c_{\mathbf{k}, j, \mu}, \quad (12)$$

$$c_{\mathbf{k}, \zeta} \equiv \sum_{j, \mu} u_{\zeta}^{j, \mu} c_{\mathbf{k}, j, \mu} = \sum_{j, \mu} \left\langle 1, m_{\zeta}; \frac{1}{2}, \sigma_{\zeta} \left| j, \mu \right. \right\rangle c_{\mathbf{k}, j, \mu}, \quad (13)$$

where n^{3d} is the $3d$ -electron-number matrix. j and μ are the eigenvalues of the total angular momentum and its z component in each $2p$ state, respectively. The unitary transformation from $\zeta = (m_{\zeta}, \sigma_{\zeta})$ to (j, μ) is obtained by the Clebsch-Gordan coefficient. Because the energy positions are not important due to the integration of emission spectra with respect to the emitted photon energy for the sum rules, specific values of \bar{V}_{pd} and $v_{\zeta \zeta', \xi \xi'}$ do not appear in the main text. In Appendix A, specific values of $v_{\zeta \zeta', \xi \xi'}$ appear in order to illustrate an example of calculated L -edge XMCPE spectra.

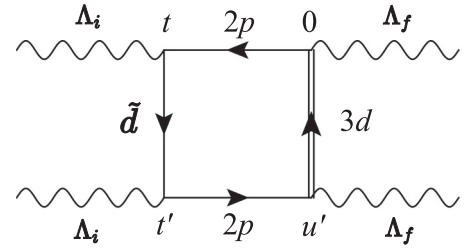


FIG. 2. Keldysh diagram for an L -edge XMCPE process. The times t and 0 belong to the $+$ leg, whereas the times t' and u' belong to the $-$ leg, as defined in Ref. [25]. The wavy lines correspond to the incident photon states labeled with Λ_i or the outgoing photon state labeled with Λ_f . The horizontal lines describe $2p$ states and the downward line indicates a free electron state denoted by \bar{d} . The upward double line indicates a $3d$ state.

B. Transition probability

To describe the transition probability from incident to outgoing photons, it is useful to use the interaction picture of H_x :

$$H_x(t) = e^{iH_0 t} H_x e^{-iH_0 t} = \sum_{\alpha, \alpha'} \sum_{\Lambda} h_{\alpha \alpha'}(t; \Lambda) a_{\Lambda} e^{-i\varepsilon_{\Lambda} t} + (\text{H.c.}), \quad (14)$$

$$h_{\alpha \alpha'}(t; \Lambda) = w_{\alpha \alpha'}(\Lambda) c_{\alpha}^\dagger(t) c_{\alpha'}(t), \quad (15)$$

$$h_{\alpha \alpha'}^\dagger(t; \Lambda) = w_{\alpha \alpha'}^*(\Lambda) c_{\alpha}^\dagger(t) c_{\alpha'}(t). \quad (16)$$

The transition probability $W_{i \rightarrow f}$ from the photon state Λ_i to Λ_f is given by the time derivative of the number of outgoing photons [24]:

$$W_{i \rightarrow f} = \left. \frac{d \langle n_{\Lambda_f} \rangle(\Lambda_i)}{dt_0} \right|_{t_0 \rightarrow \infty} = \int_{-\infty}^0 dt \int_{-\infty}^{\infty} du' \int_{-\infty}^{u'} dt' S(t, 0, u', t') e^{i\varepsilon_f(t'-t)} e^{-i\varepsilon_i u'}, \quad (17)$$

where ε_i and ε_f are the photon energies with Λ_i and Λ_f , respectively. $S(t, u, u', t')$ depending on the times t, u, u' , and t' is the S matrix, defined as follows [24,25]:

$$S(t, u, u', t') = \langle 0 | h_{\beta_1 \beta_1}^\dagger(t'; \Lambda_i) h_{\alpha_1 \alpha_1}(u'; \Lambda_f) \times h_{\alpha_2 \alpha_2}^\dagger(u; \Lambda_f) h_{\beta_2 \beta_2}(t; \Lambda_i) | 0 \rangle, \quad (18)$$

where $\langle 0 |$ and $| 0 \rangle$ correspond to the electronic ground state.

To describe an L -edge XMCPE process, we use a Keldysh diagram for the S matrix (Fig. 2). In accordance with Ref. [25], the upper and lower horizontal lines in Fig. 2 belong to the $+$ and $-$ branches, respectively. The $-$ branch corresponds to the complex conjugate of the $+$ branch, and the diagrammatic connection between the two branches provides the excitation or relaxation processes. Figure 2 shows that the incident photon with Λ_i creates a hole in the $2p$ states, which is accompanied by electron excitation from the $2p$ to \bar{d} states at the time t . After the time evolution of the $2p$ hole state from the time t to 0 , the $2p$ hole is relaxed and buried by a $3d$ electron at the time 0 , which is accompanied by the emission of the outgoing photon with Λ_f .

The expression of the S matrix corresponding to the diagram is

$$S(t, 0, u', t') = \sum_{\bar{\mathbf{K}}, \bar{\sigma}} \sum_{\mathbf{k}_d, \mathbf{k}'_d, \mathbf{k}_p, \mathbf{k}'_p} \sum_{\xi, \xi'} \sum_{\zeta, \zeta'} \sum_{\bar{\zeta}, \bar{\zeta}'} [w][G], \quad (19)$$

$$[w] = w_{\bar{\mathbf{K}}, \bar{\sigma}, \mathbf{k}_p, \zeta}^{\bar{d}, 2p}(\Lambda_i) (w_{\mathbf{k}_d \xi, \mathbf{k}'_d \xi'}^{3d, 2p}(\Lambda_f))^* \times w_{\mathbf{k}'_d \xi', \bar{\mathbf{K}}, \bar{\sigma}, \zeta}^{3d, 2p}(\Lambda_f) (w_{\bar{\mathbf{K}}, \bar{\sigma}, \mathbf{k}_p, \zeta}^{\bar{d}, 2p}(\Lambda_i))^*, \quad (20)$$

$$[G] = (-iG_{\zeta, \zeta'}^{c, 2p}(t, 0)) (-iG_{\mathbf{k}_d \xi, \mathbf{k}'_d \xi'}^{+, 3d}(0, u')) \times (-i\tilde{G}_{\bar{\zeta}, \bar{\zeta}'}^{c, 2p}(u', t')) (iG_{\bar{\mathbf{K}}}^{-, \bar{d}}(t', t)). \quad (21)$$

Each Green's function is defined as follows [25,26]:

$$G_{\alpha, \beta}^c(t, t') = \frac{1}{i} \langle T[c_\alpha(t) c_\beta^\dagger(t')] \rangle, \quad (22)$$

$$\tilde{G}_{\alpha, \beta}^c(t, t') = \frac{1}{i} \langle \tilde{T}[c_\alpha(t) c_\beta^\dagger(t')] \rangle, \quad (23)$$

$$G_{\alpha, \beta}^+(t, t') = -\frac{1}{i} \langle c_\beta^\dagger(t') c_\alpha(t) \rangle, \quad (24)$$

$$G_{\alpha, \beta}^-(t, t') = \frac{1}{i} \langle c_\alpha(t) c_\beta^\dagger(t') \rangle, \quad (25)$$

$$G_\alpha(t, t') \equiv G_{\alpha, \alpha}(t, t'). \quad (26)$$

Here, T (\tilde{T}) is the time-ordering (anti-time-ordering) operator. Because $h_{\bar{d}}$ and \bar{H}_{2p} are already diagonal, $G^{-, \bar{d}}$, $G^{c, 2p}$, and $\tilde{G}^{c, 2p}$ can be expressed as

$$iG_{\bar{\mathbf{K}}}^{-, \bar{d}}(t', t) = e^{-i\varepsilon_{\bar{\mathbf{K}}}(t'-t)}, \quad (27)$$

$$-iG_{\zeta, \zeta'}^{c, 2p}(t, 0) = \theta(0-t) \sum_{j, \mu} u_{\zeta'}^{j, \mu} u_{\zeta}^{j, \mu*} e^{-i\varepsilon_{j, \mu}(t-0)}, \quad (28)$$

$$-i\tilde{G}_{\bar{\zeta}, \bar{\zeta}'}^{c, 2p}(u', t') = \theta(u'-t') \sum_{\bar{j}, \bar{\mu}} u_{\bar{\zeta}'}^{\bar{j}, \bar{\mu}} u_{\bar{\zeta}}^{\bar{j}, \bar{\mu}*} e^{-i\varepsilon_{\bar{j}, \bar{\mu}}(u'-t')}, \quad (29)$$

where θ is the step function arising from the time-ordering and anti-time-ordering operators. Here, the inverse Fourier transform of a Green's function G is defined as

$$G(t, t') = \int_{-\infty}^{\infty} \frac{d\omega}{2\pi} G(\omega) e^{-i\omega(t-t')}. \quad (30)$$

The following relations are useful to derive the sum rules:

$$\int_{-\infty}^{\infty} \frac{d\omega_d}{2\pi} (-iG_{\mathbf{k}_d \xi, \mathbf{k}'_d \xi'}^{+, 3d}(\omega_d)) = \langle c_{\mathbf{k}'_d \xi'}^\dagger c_{\mathbf{k}_d \xi} \rangle, \quad (31)$$

$$n_{\xi}^{3d} \equiv n_{\xi, \xi}^{3d} = \frac{1}{N} \sum_{\mathbf{k}_d} \langle c_{\mathbf{k}_d, \xi}^\dagger c_{\mathbf{k}_d, \xi} \rangle. \quad (32)$$

By performing the time integrations in Eq. (17),

$$W_{i \rightarrow f} = \sum_{\bar{\mathbf{K}}, \bar{\sigma}} \sum_{\mathbf{k}_d, \mathbf{k}'_d, \mathbf{k}_p, \mathbf{k}'_p} \sum_{\xi, \xi'} \sum_{\zeta, \zeta'} \sum_{\bar{\zeta}, \bar{\zeta}'} [w] \sum_{j, \mu, \bar{j}, \bar{\mu}} u_{\zeta'}^{j, \mu} u_{\zeta}^{j, \mu*} u_{\bar{\zeta}'}^{\bar{j}, \bar{\mu}} u_{\bar{\zeta}}^{\bar{j}, \bar{\mu}*} \times \int_{-\infty}^{\infty} d\omega_d (-iG_{\mathbf{k}_d \xi, \mathbf{k}'_d \xi'}^{+, 3d}(\omega_d)) \delta(\varepsilon_{\bar{\mathbf{K}}} - \varepsilon_{if}(\omega_d)) \times \frac{1}{\varepsilon_f + \varepsilon_{j, \mu} - \omega_d + i\Gamma_p} \frac{1}{\varepsilon_f + \varepsilon_{\bar{j}, \bar{\mu}} - \omega_d - i\Gamma_p}, \quad (33)$$

$$\varepsilon_{if}(\omega_d) = \omega_d + \varepsilon_i - \varepsilon_f, \quad (34)$$

where Γ_p is for a lifetime broadening of a $2p$ core hole. In Eq. (33), it is assumed that the L_2 and L_3 edges are well separated from each other.

We adopt the following approximations in order to calculate $[w]$: (i) the dipole approximation; (ii) neglecting the s component of the photoelectron states; (iii) $\sum_{\bar{\mathbf{K}}} f(\bar{\mathbf{K}}) \Delta \bar{K} \approx \sum_{\bar{\mathbf{k}}} \int d\tilde{\mathbf{G}} f(\tilde{\mathbf{G}})$ for any function f when $\tilde{\mathbf{G}} \gg \tilde{\mathbf{k}}$; (iv) the m -independent one-body radial wave functions. These approximations lead to the following expression:

$$W_{i \rightarrow f} = \sum_j W_{i \rightarrow f}^j, \quad (35)$$

$$W_{i \rightarrow f}^j \propto \sum_{\bar{\sigma}} \sum_{\xi, \xi'} \sum_{m_p, m'_p, \bar{m}_p, \bar{m}'_p} \sum_{\mu, \bar{\mu}} M_{\bar{m}'_p, m'_p}^{\bar{d}, 2p}(\lambda_i, \beta_i) \times M_{m_\xi, m'_p}^{3d, 2p}(\lambda_f, \beta_f) M_{\bar{m}'_p, \bar{m}_p}^{3d, 2p}(\lambda_f, \beta_f) \times u_{m_p, \bar{\sigma}}^{j, \mu} u_{m'_p, \sigma_\xi}^{j, \mu*} u_{\bar{m}_p, \sigma_{\xi'}}^{j, \bar{\mu}} u_{\bar{m}'_p, \bar{\sigma}}^{j, \bar{\mu}*} \times \int_{-\infty}^{\infty} d\omega_d \left(-i \sum_{\mathbf{k}_d} G_{\mathbf{k}_d \xi, \mathbf{k}'_d \xi'}^{+, 3d}(\omega_d) \right) \times \frac{1}{\varepsilon_f + \varepsilon_{j, \mu} - \omega_d + i\Gamma_p} \frac{1}{\varepsilon_f + \varepsilon_{j, \bar{\mu}} - \omega_d - i\Gamma_p}, \quad (36)$$

where β_i and β_f are incident and emitted x-ray angles with respect to the magnetization direction, respectively. It should be mentioned that for the linear polarization ($\lambda_{i(f)} = 0$) $\beta_{i(f)}$ corresponds to the angle between the polarization and magnetization directions, while for circular polarization ($\lambda_{i(f)} = \pm 1$) $\beta_{i(f)}$ corresponds to the angle between the photon propagation and magnetization directions. The dependence on β_i and β_f is introduced by $M^{\bar{d}, 2p}$ and $M^{3d, 2p}$, respectively:

$$M_{m', m}^{\bar{d}, 2p}(\lambda_i, \beta_i) = \sum_{\bar{m}} G(1, m'; 1, \bar{m} - m' | 2, \bar{m}) d_{\bar{m} - m', \lambda_i}^{(1)}(\beta_i) \times G(1, m; 1, \bar{m} - m | 2, \bar{m}) d_{\bar{m} - m, \lambda_i}^{(1)}(\beta_i), \quad (37)$$

$$M_{m_d, m_p}^{3d, 2p}(\lambda_f, \beta_f) = G(1, m_p; 1, m_d - m_p | 2, m_d) d_{m_d - m_p, \lambda_f}^{(1)}(\beta_f), \quad (38)$$

$$G(l_1, m_1; l_2, m_2 | l_3, m_3) = \int d\hat{\mathbf{r}} Y_{l_3 m_3}^*(\hat{\mathbf{r}}) Y_{l_2 m_2}(\hat{\mathbf{r}}) Y_{l_1 m_1}(\hat{\mathbf{r}}), \quad (39)$$

where Y is the spherical harmonic function and $d^{(1)}$ is the orthogonal Wigner's small d matrix for the first order. While calculated L -edge XMCP spectra by using Eq. (36) are shown in Appendix A, details of the derivation of Eq. (36) are explained in Appendix B.

When $2p \rightarrow \bar{s}$ transitions, where \bar{s} is the s state of a photoelectron, are considered exactly, theoretical formulation becomes much more complicated. Indeed, the $2p \rightarrow \bar{s}$ contribution can depend on the incident x-ray energy and the photoelectron kinetic energy in experimental settings. For example, photoelectron energy of a few kiloelectronvolts can make the \bar{s} contribution negligible, but too high photoelectron energy recovers the \bar{s} contribution. Thus the deviation caused

by neglecting the transitions should be checked with experimental data in future.

For sum rules, $W_{i \rightarrow f}^j$ is integrated with respect to the x-ray emission energy, which leads to

$$\begin{aligned} I_{\lambda_i, \lambda_f}^j(\beta_i, \beta_f) &\equiv \int d\varepsilon_f W_{i \rightarrow f}^j \\ &\propto \sum_{\tilde{\sigma}} \sum_{\xi, \xi'} \sum_{m_p, m'_p} \sum_{\tilde{m}_p, \tilde{m}'_p} \sum_{\mu, \tilde{\mu}} M_{\tilde{m}'_p, m_p}^{\tilde{d}, 2p}(\lambda_i, \beta_i) \\ &\quad \times M_{m_\xi, m'_p}^{3d, 2p}(\lambda_f, \beta_f) M_{m_{\xi'}, \tilde{m}'_p}^{3d, 2p}(\lambda_f, \beta_f) \\ &\quad \times u_{m_p, \tilde{\sigma}}^{j, \mu} u_{m'_p, \sigma_\xi}^{j, \mu*} u_{\tilde{m}_p, \sigma_{\xi'}}^{j, \tilde{\mu}} u_{\tilde{m}'_p, \tilde{\sigma}}^{j, \tilde{\mu}*} n_{\xi', \xi}^{3d}. \end{aligned} \quad (40)$$

In order to derive Eq. (40), it is assumed that $|\varepsilon_{j, \mu} - \varepsilon_{j, \tilde{\mu}}| \gg \Gamma_p$. Although the opposite limit $|\varepsilon_{j, \mu} - \varepsilon_{j, \tilde{\mu}}| \ll \Gamma_p$ gives Eq. (40) with $\mu = \tilde{\mu}$ in any β_i and β_f , this difference does not appear in $\beta_i = \beta_f = 0$. For 3d TMs, the spin-orbit coupling in the 3d states is not pronounced compared with the Coulomb interaction, which gives $n_{\xi', \xi}^{3d} \approx n_{\xi', \xi}^{3d} \delta_{\sigma_{\xi'}, \sigma_\xi}$.

C. Sum rules

In this subsection, we restrict the sum rules of L -edge XMCPE for 3d TMs to those for $\beta_i = \beta_f = 0$, where only the diagonal components n_{ξ}^{3d} appear. The detailed reason for the appearance of n_{ξ}^{3d} is as follows: $M_{\tilde{m}'_p, m_p}^{\tilde{d}, 2p}(\lambda_i, 0)$ first gives $\tilde{m}'_p = m_p$, which leads to $\tilde{\mu} = \mu$ because of $u_{m_p, \tilde{\sigma}}^{j, \mu} u_{m_p, \tilde{\sigma}}^{j, \mu*}$. Since $\sigma_{\xi'} = \sigma_\xi$, $u_{m'_p, \sigma_\xi}^{j, \mu*} u_{\tilde{m}_p, \sigma_\xi}^{j, \mu}$ gives $m'_p = \tilde{m}_p$, which leads to $m_\xi = m_{\xi'}$ due to $M_{m_\xi, m'_p}^{3d, 2p}(\lambda_f, 0) M_{m_{\xi'}, \tilde{m}'_p}^{3d, 2p}(\lambda_f, 0)$. In Sec. III, we discuss the cases for arbitrary β_i and β_f .

The following characteristic functions are useful to derive sum rules analytically:

$$\chi_{\pm 2}(m) = \frac{m}{2} \left(\frac{m^2 - 1}{3} \right) \left(\frac{m \pm 2}{4} \right), \quad (41)$$

$$\chi_{\pm 1}(m) = m \left(\frac{m \pm 1}{2} \right) \left(\frac{4 - m^2}{3} \right), \quad (42)$$

$$\chi_0(m) = (1 - m^2) \left(\frac{4 - m^2}{4} \right), \quad (43)$$

$$\chi_{\pm 1/2}(\sigma) = \frac{1}{2} \pm \sigma, \quad (44)$$

$$1 = \sum_{m'=-2}^2 \chi_{m'}(m) = \sum_{\sigma'=\pm 1/2} \chi_{\sigma'}(\sigma). \quad (45)$$

The derivation of $\chi_{m'}(m)$ is discussed in Appendix C. In addition, the Gaunt integral defined in Eq. (39) is proportional to the Clebsch-Gordan coefficient for given azimuthal quantum numbers l_1 , l_2 , and l_3 :

$$G(l_1, m_1; l_2, m_2 | l_3, m_3) \propto \langle l_1, m_1; l_2, m_2 | l_3, m_3 \rangle. \quad (46)$$

The following replacements make coefficients appearing in equations simpler:

$$\langle l, m; 1, \tilde{m} | l', m' \rangle^2 \rightarrow (2l + 1)(2l + 2) \langle l, m; 1, \tilde{m} | l', m' \rangle^2, \quad (47)$$

$$\langle l, m; 1/2, \sigma | l', m' \rangle^2 \rightarrow (2l + 1) \langle l, m; 1/2, \sigma | l', m' \rangle^2. \quad (48)$$

By using these functions, the representation of $I_{\lambda_i, \lambda_f}^j (\equiv I_{\lambda_i, \lambda_f}^j(0, 0))$ can keep summation for m and σ , shown as follows:

$$\begin{aligned} I_{0, \pm}^{L_3} &\propto \sum_{m, \sigma} (-6m^4 + 32m^3\sigma \mp 6m^3 \pm 64m^2\sigma \\ &\quad \pm 62m^2 - 32m\sigma \pm 138m \mp 64\sigma + 76)n_{m\sigma}^{3d}, \end{aligned} \quad (49)$$

$$I_{0, 0}^{L_3} \propto \sum_{m, \sigma} (12m^4 - 64m^3\sigma - 136m^2 + 256m\sigma + 352)n_{m\sigma}^{3d}, \quad (50)$$

$$\begin{aligned} I_{\pm, \pm}^{L_3} &\propto \sum_{m, \sigma} (\pm 20m^4\sigma + 3m^4 + 64m^3\sigma \pm 28m^3 \pm 48m^2\sigma \\ &\quad + 79m^2 - 4m\sigma \pm 86m \mp 8\sigma + 32)n_{m\sigma}^{3d}, \end{aligned} \quad (51)$$

$$\begin{aligned} I_{\mp, \pm}^{L_3} &\propto \sum_{m, \sigma} (\mp 20m^4\sigma + 3m^4 + 24m^3\sigma \mp 22m^3 \pm 128m^2\sigma \\ &\quad - 21m^2 - 84m\sigma \pm 136m \mp 168\sigma + 132)n_{m\sigma}^{3d}, \end{aligned} \quad (52)$$

$$\begin{aligned} I_{\pm, 0}^{L_3} &\propto \sum_{m, \sigma} (\mp 40m^4\sigma - 6m^4 - 88m^3\sigma \mp 50m^3 \pm 120m^2\sigma \\ &\quad - 52m^2 + 352m\sigma \pm 200m \pm 160\sigma + 304)n_{m\sigma}^{3d}, \end{aligned} \quad (53)$$

where the superscript L_3 indicates $j = 3/2$ for the $2p$ states. For L_2 or $j = 1/2$,

$$\begin{aligned} I_{0, \pm}^{L_2} &\propto \sum_{m, \sigma} (-40m^3\sigma \mp 80m^2\sigma + 20m^2 + 40m\sigma \pm 60m \\ &\quad \pm 80\sigma + 40)n_{m\sigma}^{3d}, \end{aligned} \quad (54)$$

$$I_{0, 0}^{L_2} \propto \sum_{m, \sigma} (80m^3\sigma - 40m^2 - 320m\sigma + 160)n_{m\sigma}^{3d}, \quad (55)$$

$$\begin{aligned} I_{\pm, \pm}^{L_2} &\propto \sum_{m, \sigma} (\mp 40m^4\sigma - 80m^3\sigma \pm 10m^3 \pm 60m^2\sigma \\ &\quad + 40m^2 + 140m\sigma \pm 50m \pm 40\sigma + 20)n_{m\sigma}^{3d}, \end{aligned} \quad (56)$$

$$\begin{aligned} I_{\mp, \pm}^{L_2} &\propto \sum_{m, \sigma} (\pm 40m^4\sigma \mp 10m^3 \mp 220m^2\sigma - 60m\sigma \pm 70m \\ &\quad \pm 120\sigma + 60)n_{m\sigma}^{3d}, \end{aligned} \quad (57)$$

$$\begin{aligned} I_{\pm, 0}^{L_2} &\propto \sum_{m, \sigma} (\pm 80m^4\sigma + 80m^3\sigma \mp 20m^3 \mp 360m^2\sigma \\ &\quad - 40m^2 - 320m\sigma \pm 80m \pm 160\sigma + 160)n_{m\sigma}^{3d}. \end{aligned} \quad (58)$$

Adding most of the polarization components gives a relation with the total 3d electron number $n_{3d} (= \sum_{m\sigma} n_{m\sigma}^{3d})$ and a z -component spin-orbit term $\langle L_z S_z \rangle$:

$$\begin{aligned} I_{LS}^{L_3} &\equiv \sum_{\lambda_i, \lambda_f} I_{\lambda_i, \lambda_f}^{L_3} \\ &\propto 720 \sum_{m, \sigma} (m\sigma + 2)n_{m, \sigma} = 720(2n_{3d} + \langle L_z S_z \rangle), \end{aligned} \quad (59)$$

$$I_{LS}^{L_2} \equiv \sum_{\lambda_i, \lambda_f} \lambda_i^2 I_{\lambda_i, \lambda_f}^{L_2} = 2 \sum_{\lambda_f} I_{0, \lambda_f}^{L_2} \propto 480(n_{3d} - \langle L_z S_z \rangle), \quad (60)$$

$$I_n \equiv 2I_{LS}^{L_3} + 3I_{LS}^{L_2} \propto 1440 \times 3 n_{3d}, \quad (61)$$

$$I_{LS} \equiv I_{LS}^{L_3} - 3I_{LS}^{L_2} \propto 720 \times 3 \langle L_z S_z \rangle, \quad (62)$$

$$\frac{I_{LS}}{I_n} = \frac{1}{2} \frac{\langle L_z S_z \rangle}{n_{3d}}, \quad (63)$$

where $\langle L_z S_z \rangle = \sum_{m,\sigma} m\sigma n_{m,\sigma}^{3d}$. Here, we define circular dichroism of x-ray emission:

$$\Delta I_{\lambda_i} \equiv \sum_{\lambda_f} \lambda_f I_{\lambda_i, \lambda_f} = I_{\lambda_i, +} - I_{\lambda_i, -}. \quad (64)$$

By using ΔI terms, a sum rule for a z -component angular momentum $\langle L_z \rangle$ is obtained:

$$\begin{aligned} I_L &\equiv \sum_{\lambda_i} (2\Delta I_{\lambda_i}^{L_3} + 3\lambda_i^2 \Delta I_{\lambda_i}^{L_2}) = 2 \sum_{\lambda_i} \Delta I_{\lambda_i}^{L_3} + 6\Delta I_0^{L_2} \\ &\propto 2160 \sum_{m,\sigma} mn_{m,\sigma} = 2160 \langle L_z \rangle, \end{aligned} \quad (65)$$

$$\frac{I_L}{I_n} = \frac{1}{2} \frac{\langle L_z \rangle}{n_{3d}}. \quad (66)$$

A sum rule for a linear combination of z -component magnetic dipole and spin terms ($\langle T_z \rangle$ and $\langle S_z \rangle$) is also obtained with a similar manner for $\langle L_z \rangle$:

$$\begin{aligned} I_{TS}^{(1)} &\equiv \sum_{\lambda_i} (\Delta I_{\lambda_i}^{L_3} - 3\lambda_i^2 \Delta I_{\lambda_i}^{L_2}) = \sum_{\lambda_i} \Delta I_{\lambda_i}^{L_3} - 6\Delta I_0^{L_2} \\ &\propto 1440 \sum_{m,\sigma} (m^2\sigma - \sigma) n_{m,\sigma}^{3d} \\ &= 720[7 \langle T_z \rangle + 2 \langle S_z \rangle], \end{aligned} \quad (67)$$

$$\langle T_z \rangle = \frac{2}{7} \sum_{m,\sigma} (m^2 - 2)\sigma n_{m,\sigma}^{3d}, \quad (68)$$

$$\langle S_z \rangle = \sum_{m,\sigma} \sigma n_{m,\sigma}^{3d}, \quad (69)$$

$$\frac{I_{TS}^{(1)}}{I_n} = \frac{1}{n_{3d}} \left(\frac{7}{6} \langle T_z \rangle + \frac{1}{3} \langle S_z \rangle \right). \quad (70)$$

Note that the expression of $\langle T_z \rangle$ in Eq. (68) is only valid for d states [10].

By taking only circularly polarized emission terms, a sum rule for a z -component quadrupole term $\langle Q_{zz} \rangle$ can be found:

$$\begin{aligned} I_Q &\equiv \sum_{\lambda_i, \lambda_f} \lambda_f^2 (10I_{\lambda_i, \lambda_f}^{L_3} + (3\lambda_i^2 + 8)I_{\lambda_i, \lambda_f}^{L_2}) \\ &\propto 3600 \sum_{m,\sigma} (m^2 + 2)n_{m,\sigma}^{3d} \\ &= 1800(7 \langle Q_{zz} \rangle + 8 n_{3d}), \end{aligned} \quad (71)$$

$$\langle Q_{zz} \rangle = \frac{2}{7} \sum_{m,\sigma} (m^2 - 2)n_{m,\sigma}^{3d}, \quad (72)$$

$$\frac{I_Q}{I_n} = \frac{35}{12} \frac{\langle Q_{zz} \rangle}{n_{3d}} + \frac{10}{3}. \quad (73)$$

Next, we derive a sum rule only for S_z (or T_z) by finding another relation with T_z and S_z with a linear combination

different from that in $I_{TS}^{(1)}$. The basic strategy to obtain the sum rule is elimination of m and m^3 terms by linear combinations. As useful linear combinations, we can take the following combinations which have the same m terms:

$$\sum_{\lambda_i} \lambda_i^2 \Delta I_{\lambda_i}^{L_3} \propto \sum_{m,\sigma} (12m^3 + 352m^2\sigma + 444m - 352\sigma) n_{m,\sigma}^{3d}, \quad (74)$$

$$\begin{aligned} \sum_{\lambda} \lambda (2I_{\lambda, \lambda}^{L_3} + I_{\lambda, \lambda}^{L_2}) &\propto \sum_{m,\sigma} (132m^3 + 312m^2\sigma + 444m \\ &\quad + 48\sigma) n_{m,\sigma}^{3d}, \end{aligned} \quad (75)$$

$$\begin{aligned} I_1 &\equiv \sum_{\lambda_i} \lambda_i^2 \Delta I_{\lambda_i}^{L_3} - \sum_{\lambda} \lambda (2I_{\lambda, \lambda}^{L_3} + I_{\lambda, \lambda}^{L_2}) \\ &\propto \sum_{m,\sigma} (-120m^3 + 40m^2\sigma - 400\sigma) n_{m,\sigma}^{3d}. \end{aligned} \quad (76)$$

We can also take the following combination which has the same m^3 term as I_1 :

$$10\Delta I_0^{L_3} - 23\Delta I_0^{L_2} \propto \sum_{m,\sigma} (-120m^3 + 4960m^2\sigma - 4960\sigma) n_{m,\sigma}^{3d}, \quad (77)$$

$$\begin{aligned} I_{TS}^{(2)} &\equiv (10\Delta I_0^{L_3} - 23\Delta I_0^{L_2}) - I_1 \\ &\propto 120 \sum_{m,\sigma} (41m^2\sigma - 38\sigma) n_{m,\sigma}^{3d} \\ &= 60(41 \times 7 \langle T_z \rangle + 44 \times 2 \langle S_z \rangle). \end{aligned} \quad (78)$$

A linear combination of $I_{TS}^{(1)}$ and $I_{TS}^{(2)}$ eliminates the $\langle T_z \rangle$ ($\langle S_z \rangle$) terms and gives a sum rule only for $\langle S_z \rangle$ ($\langle T_z \rangle$):

$$I_S \equiv 41I_{TS}^{(1)} - 12I_{TS}^{(2)} \propto -4320 \langle S_z \rangle, \quad (79)$$

$$\frac{I_S}{I_n} = -\frac{\langle S_z \rangle}{n_{3d}}, \quad (80)$$

$$I_T \equiv 11I_{TS}^{(1)} - 3I_{TS}^{(2)} \propto 540 \times 7 \langle T_z \rangle, \quad (81)$$

$$\frac{I_T}{I_n} = \frac{7 \langle T_z \rangle}{8 n_{3d}}. \quad (82)$$

Because the individual sum rules for $\langle S_z \rangle$ and $\langle T_z \rangle$ cannot be obtained by XMCD, those are an advantage of L -edge XMCDPE.

The following linear combination gives another relation with T_z and S_z different from $I_{TS}^{(1)}$ and $I_{TS}^{(2)}$:

$$\begin{aligned} \sum_{\lambda} \lambda (2I_{-\lambda, \lambda}^{L_3} + I_{-\lambda, \lambda}^{L_2}) \\ \propto \sum_{m,\sigma} (-108m^3 + 72m^2\sigma + 684m - 432\sigma) n_{m,\sigma}^{3d}. \end{aligned} \quad (83)$$

By combining Eqs. (75) and (83),

$$\begin{aligned} I_2 &\equiv \sum_{\lambda} \lambda [57(2I_{\lambda, \lambda}^{L_3} + I_{\lambda, \lambda}^{L_2}) - 37(2I_{-\lambda, \lambda}^{L_3} + I_{-\lambda, \lambda}^{L_2})] \\ &\propto 720 \sum_{m,\sigma} (16m^3 + 21m^2\sigma + 26\sigma) n_{m,\sigma}^{3d}, \end{aligned} \quad (84)$$

$$\begin{aligned}
I_{TS}^{(3)} &\equiv 96I_1 + I_2 \\
&\propto 240 \sum_{m,\sigma} (79m^2\sigma - 82\sigma)n_{m\sigma}^{3d} \\
&= 120(79 \times 7 \langle T_z \rangle + 76 \times 2 \langle S_z \rangle). \quad (85)
\end{aligned}$$

Although $I_{TS}^{(3)}$ gives a sum rule only for S_z (or T_z), the linear combination in Eq. (80) is simpler than that in a sum rule by $I_{TS}^{(3)}$.

In Appendix A, the values obtained by using the sum rules and those obtained directly from density of states within the Hartree-Fock approximation are compared as an example.

III. ANGULAR DEPENDENCE OF INTEGRAL VALUES OF SPECTRA

In Sec. II C, β_i and β_f are fixed to zero, which leads to the sum rules only using $n_{m\sigma}^{3d}$. When β_i and β_f are taken to arbitrary angles, off-diagonal components of n^{3d} appear generally in the sum rule derivation. Although in atomic systems n^{3d} is diagonal to the magnetic quantum numbers m , in solids n^{3d} can be diagonal to real orbitals γ :

$$n_{m'\sigma, m\sigma}^{3d} = \sum_{\gamma} u_m^{\gamma} n_{\gamma\sigma}^{3d} u_{m'}^{\gamma*}. \quad (86)$$

In a cubic system, γ corresponds to xy , yz , zx , x^2 ($\equiv x^2 - y^2$) and z^2 ($\equiv 3x^2 - z^2$). The matrix elements u_m^{γ} of the unitary transformation for a cubic system are given by

$$u_{\pm 2}^{xy} = \mp \frac{i}{\sqrt{2}}, \quad (87)$$

$$u_{\pm 2}^{x^2} = \frac{1}{\sqrt{2}}, \quad (88)$$

$$u_{\pm 1}^{yz} = \frac{i}{\sqrt{2}}, \quad (89)$$

$$u_{\pm 1}^{zx} = \mp \frac{i}{\sqrt{2}}, \quad (90)$$

$$u_0^{z^2} = 1. \quad (91)$$

The other elements are zero. In this section, we investigate the angular dependence of sum rules by using the unitary transformation and numerical calculations.

In order to investigate the angular dependence, we replace I , which is defined in Eq. (40) and used to derive the sum rules, by the following intensity:

$$\begin{aligned}
I_{\lambda_i, \lambda_f}^{j, \gamma, \sigma_d}(\beta_i, \beta_f) &\equiv \sum_{m_d, m'_d} \sum_{m_p, m'_p} \sum_{\tilde{m}_p, \tilde{m}'_p} \sum_{\sigma_p} \sum_{\mu, \tilde{\mu}} M_{\tilde{m}'_p, m_p}^{\tilde{d}, 2p}(\lambda_i, \beta_i) \\
&\times M_{m_d, m'_p}^{3d, 2p}(\lambda_f, \beta_f) M_{m'_d, \tilde{m}_p}^{3d, 2p}(\lambda_f, \beta_f) \\
&\times u_{m_p, \sigma_p}^{j, \mu} u_{m'_p, \sigma_d}^{j, \mu*} u_{\tilde{m}_p, \sigma_d}^{j, \tilde{\mu}} u_{\tilde{m}'_p, \sigma_p}^{j, \tilde{\mu}*} u_{m'_d}^{\gamma} u_{m_d}^{\gamma*}. \quad (92)
\end{aligned}$$

This intensity reflects the situation where only the orbital specified by γ and σ_d is occupied in the $3d$ shell. For example, $I^{xy, \uparrow}$ means I with $n_{\gamma\sigma_d}^{3d} = \delta_{\gamma, xy} \delta_{\sigma_d, \uparrow}$.

We found that our numerical calculations show no β_i and β_f dependence of I_n . This indicates that the angular dependence of the sum rules where the denominator is I_n is determined by the numerator. Figures 3 and 4 show that $I_{TS}^{(1)}$

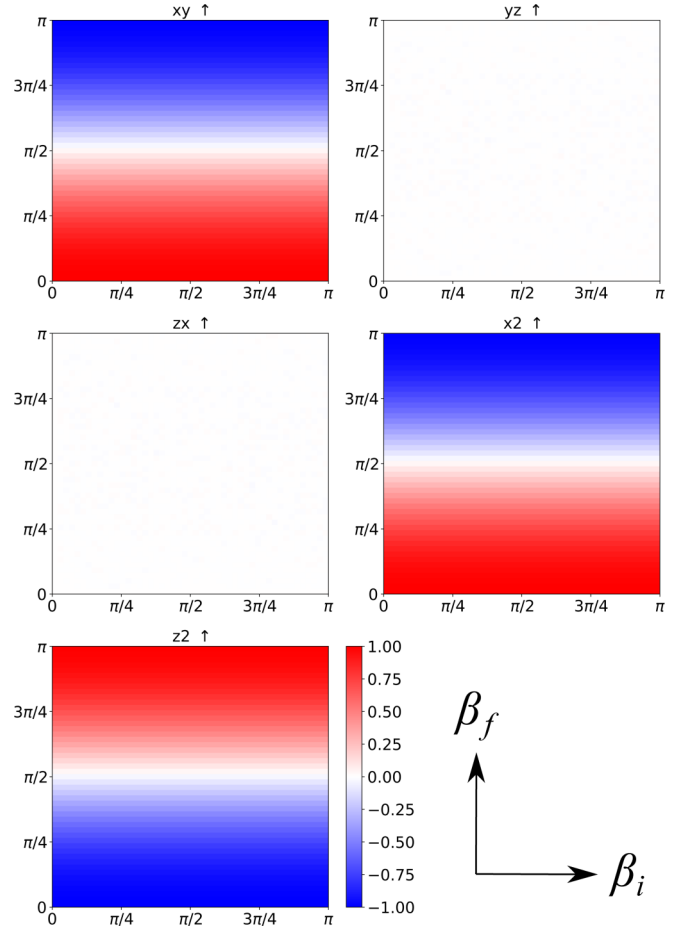


FIG. 3. Angular dependence of $I_{TS}^{(1)}$ defined in Eq. (67) with up spin and each orbital. The horizontal and vertical axes indicate the values of β_i and β_f , respectively. The values of $I_{TS}^{(1)}$ with each orbital are normalized by the maximum value found in the (β_i, β_f) space.

and I_Q have cosinusoidal dependence on β_f . In Figs. 3 and 4, the angular dependence is normalized by each maximum value found in the (β_i, β_f) space for each orbital and up spin state. Note that the zero values of $I_{TS}^{(1)}$ with yz and zx orbitals reflect that

$$\langle T_z \rangle_{yz, \uparrow} = \langle T_z \rangle_{zx, \uparrow} = -\frac{1}{7}, \quad (93)$$

$$\langle S_z \rangle_{yz, \uparrow} = \langle S_z \rangle_{zx, \uparrow} = \frac{1}{2}, \quad (94)$$

$$\frac{7}{6} \langle T_z \rangle + \frac{1}{3} \langle S_z \rangle = 0. \quad (95)$$

Because the rotations at β_i and β_f are in the y axis, there is no angular dependence of I_Q with the zx orbital.

Figure 5 shows the angular dependence of I_S/I_n (not only I_S) with up spin and each γ without normalization. Although the angular dependence of I_n , $I_{TS}^{(1)}$, and I_Q is similar to that in x-ray absorption spectroscopy, the angular dependence of I_S/I_n is difficult to express by the trigonometric functions. In Fig. 5, the value of $-1/2$ is correctly obtained for up spin and all orbitals at $(\beta_i, \beta_f) = (0, 0)$ [see Eq. (80)]. In addition, the value of $1/2$ is obtained at $(\beta_i, \beta_f) = (\pi, \pi)$, which can be interpreted by setting the opposite magnetization. However, regions where the absolute value of I_S/I_n becomes greater

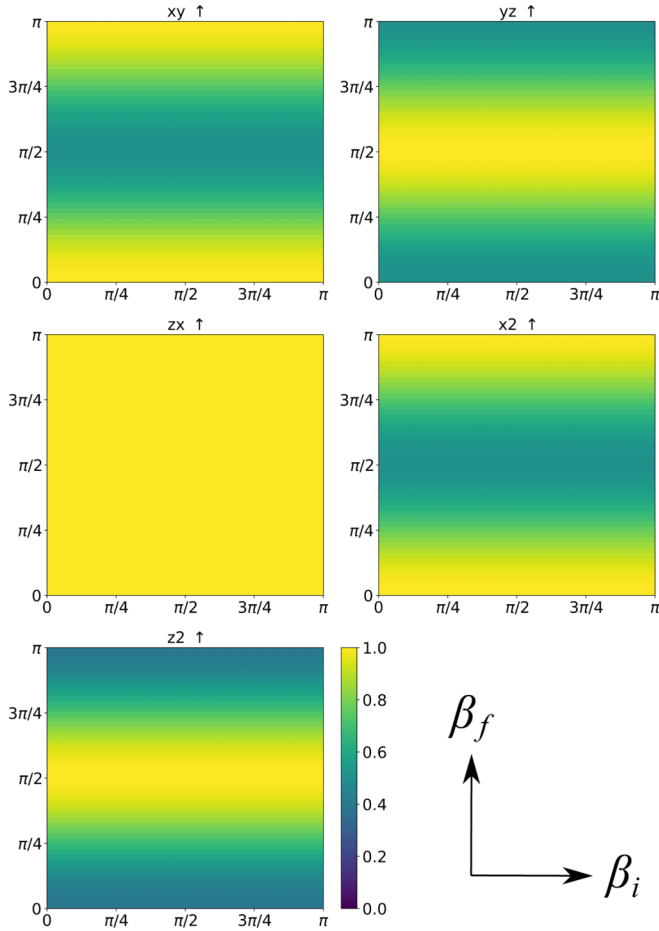


FIG. 4. Angular dependence of I_Q defined in Eq. (71) with up spin and each orbital. The horizontal and vertical axes indicate the values of β_i and β_f , respectively. The values of I_Q with each orbital are normalized by the maximum value found in the (β_i, β_f) space.

than a half appear except for the zx orbital, indicating that the sum rule for S_z is not valid in arbitrary β_i and β_f . In general electronic structure, the angular dependence for up and down spin is obtained by the linear combination of the dependence for each orbital. Thus the sum rule for S_z can be used only $(\beta_i, \beta_f) \approx (0, 0), (\pi, \pi)$. Because the sum rule for T_z is the counterpart of that for S_z as shown in Eqs. (79) and (81), the angular dependence for T_z has the same tendencies of that for S_z .

It should be mentioned that the sign in Figs. 3 and 5 becomes completely opposite in the down-spin cases. Thus an orbital occupied by two electrons with different spins does not contribute to $I_{TS}^{(1)}$ and I_S , which agrees with our physical intuition for the nonmagnetic systems correctly.

IV. DISCUSSION

Generally, we cannot derive the explicit sum rules with the (m, σ) -off-diagonal components which do not connect with expectation values of physical quantities. Indeed, I^{yz} and I^{zx} have off-diagonal components with $(m, m') = (\pm 1, \mp 1)$ (shown in Figs. S20–S23 and S25–S28 in the Supplemental Material [27]). Furthermore, although the I^z component has

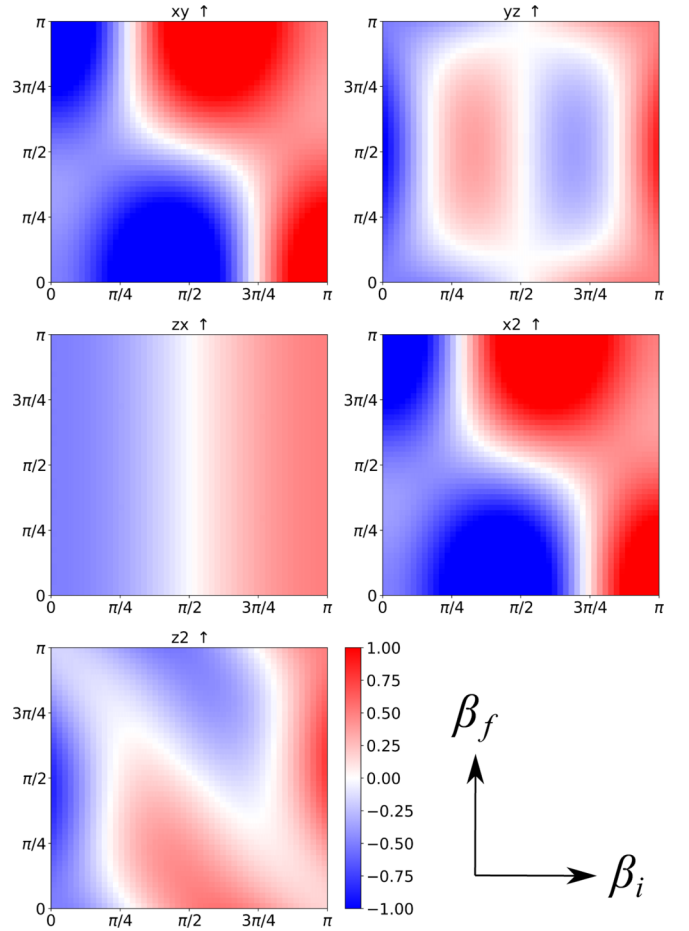


FIG. 5. Angular dependence of I_S/I_n defined in Eq. (80) with up spin and each orbital. The horizontal and vertical axes indicate the values of β_i and β_f , respectively.

no (m, σ) -off-diagonal component, its angular dependence is complicated (shown in Figs. S9 and S10 in the Supplemental Material [27]). In addition, in the practical cases, the energy splitting of the $2p$ sublevels $|\varepsilon_{j,\mu} - \varepsilon_{j,\bar{\mu}}|$ is not far from the lifetime Γ_p , which makes the contribution of the μ -off-diagonal components incomplete (the angular dependence of the μ -off-diagonal terms are shown in Figs. S11–S18 in the Supplemental Material [27]). In the XMCD cases, the initial $2p$ states are fully occupied, and thus the angular dependence of XMCD is determined by the transition matrix element from $2p$ to $3d$ states, and just cosinusoidal. On the other hand, in XMCPe the incident photon prepares a $2p$ hole state to accept a $3d$ electron, which causes the additional transition matrix element and complex angular dependence of XMCPe compared with XMCD.

Nevertheless, I_n , $I_{TS}^{(1)}$, and I_Q have much simpler angular dependence than I_S (or I_T). This shows that the off-diagonal components are canceled in arbitrary β_i and β_f by the linear combination of the intensity $I_{\lambda_i, \lambda_f}^j$ in I_n , $I_{TS}^{(1)}$, and I_Q . On the other hand, some off-diagonal components remain in the linear combination given by Eqs. (80) and (82), and thus I_S/I_n and I_T/I_n cannot keep the sum rule relation in the whole space of (β_i, β_f) .

We briefly comment on the practical application of the XMCPE sum rules. Because the derived sum rules require the ideal intensity ratio between the L_2 and L_3 edges, the effects of self-absorption should be eliminated from observed spectra. In particular, the L_2 -edge emission intensity suffers more from the self-absorption effect than the L_3 -edge one because x rays emitted by the transition from $3d$ to $2p_{1/2}$ states can be absorbed by $2p_{3/2}$ core electrons. This absorption deviates the intensity ratio, which causes errors in the values of the physical quantities estimated by using the sum rules. How much each approximation is satisfied also affects the estimated values by the sum rules. For instance, the deviation of $u_{m,\sigma}^{j,\mu}$ from the Clebsch-Gordan coefficient shifts the calculated value of I_S/I_n from the true value of $\langle S_z \rangle / n_{3d}$ (see Appendix A). In addition, in order to observe XMCPE in the soft x-ray region, a device which separates the helicity of the emitted x rays is required. In the K -edge XMCPE measurement, a quarter-wave plate of a single-crystal diamond plate has been used to convert circularly polarized x rays to linearly polarized x rays [23,28]. As far as we know, such devices have not been achieved in the soft x-ray region, and thus the sum rules are awaiting future experimental confirmation.

V. CONCLUSION

We have proposed the sum rules of L -edge XMCPE for $3d$ TMs by use of the Keldysh Green's function approach. The sum rules make use of the incident and emitted x-ray photon helicities, which provide the $3d$ expectation values related to L_z , Q_{zz} , T_z , and S_z . In particular, the individual sum rules for the S_z and T_z terms are unique compared with the sum rules in x-ray absorption spectroscopy such as XMCD.

In the derivation of the sum rules, we assumed that spin-orbit interaction for d electron states is small. Moreover, it was assumed that the photoelectron energy is sufficiently large to perform summation (or integration) with respect to a crystal-momentum vector and that with respect to a reciprocal lattice vector separately. The high photoelectron energy is also related to the approximation to neglect the s component of the photoelectron. In addition, electron correlation should be moderate not to merge the L_2 and L_3 edges for using the sum rules. These assumptions could be satisfied in $3d$ TMs with high incident photon energy.

Because our individual sum rules for S_z and T_z were derived by the heuristic linear combinations of integrals of spectra, there could be other linear combinations providing different sum rules. However, the angular dependence for S_z (or T_z) shows that such linear combinations do not always keep the sum rule relations in the whole space of (β_i, β_f) . Thus the angular dependence for them should be checked carefully. The difference of sum rules between L -edge XMCD and XMCPE comes from the additional transition matrix element in the emission process, which makes the angular dependence of XMCPE spectra more complicated than that of XMCD.

Although the observation of XMCPE in the soft x-ray region has not been realized, our findings would encourage development of experimental setups.

ACKNOWLEDGMENT

This work was supported by the JSPS Grant-in-Aid for Scientific Research (B) No. 19H04405 and QST President's Strategic Grant (Exploratory Research).

APPENDIX A

In this Appendix, we show calculated L -edge XMCPE spectra of BCC iron within the Hartree-Fock approximation (or mean-field approximation) as an example. The method and parameters of the calculation is basically the same as that for K -edge XMCPE in Ref. [24]. The band Hamiltonian H_{band} is approximated to a Hubbard-type Hamiltonian \bar{H}_{band} within the Hartree-Fock approximation:

$$\bar{H}_{\text{band}} = h_{\text{TB}} + \bar{H}'_{\text{band}} - \bar{H}_{\text{band}}^{\text{TB}} = \sum_{\mathbf{k}, \gamma, \sigma} E_{\mathbf{k}\gamma\sigma} c_{\mathbf{k}, \gamma, \sigma}^\dagger c_{\mathbf{k}, \gamma, \sigma}, \quad (\text{A1})$$

$$\begin{aligned} \bar{H}'_{\text{band}} = & \sum_{\mathbf{k}, \mu, \sigma} \left\{ \frac{U}{2} [\bar{n}_\mu - \text{sgn}(\sigma) \bar{m}_\mu] \right. \\ & \left. + \sum_{\mu' (\neq \mu)} \left[\left(U' - \frac{J}{2} \right) \bar{n}_{\mu'} - \text{sgn}(\sigma) \frac{J}{2} \bar{m}_{\mu'} \right] \right\} n_{\mathbf{k}, \mu, \sigma} + \bar{E}, \end{aligned} \quad (\text{A2})$$

where μ (μ') and γ are the indices of Wannier orbitals and bands, respectively. h_{TB} is the tight-binding Hamiltonian where not only $3d$ but also $4s$ and $4p$ states are considered. The hopping parameters in h_{TB} are determined to reproduce band structures calculated by density functional theory without spin polarization. The generalized gradient approximation with the Perdew-Burke-Ernzerhof functional is used as an effective exchange-correlation functional [29]. Spin polarization is caused by the Coulomb integrals U , U' , and J in the Hamiltonian. \bar{n} and \bar{m} are the mean values of electron number and spin polarization. Here, the double counting correction $\bar{H}_{\text{band}}^{\text{TB}}$ is \bar{H}'_{band} with \bar{n} and \bar{m} obtained by solving only h_{TB} .

The explicit form of $v_{\zeta\zeta', \xi\xi'}$ is represented by the matrix elements of the electron-electron interaction v_{ee} :

$$v_{\zeta\zeta', \xi\xi'} = \langle \psi_\zeta \psi_\xi | v_{ee} | \psi_{\zeta'} \psi_{\xi'} \rangle - \langle \psi_\zeta \psi_\xi | v_{ee} | \psi_{\xi'} \psi_{\zeta'} \rangle, \quad (\text{A3})$$

$$\begin{aligned} & \langle \psi_\zeta \psi_\xi | v_{ee} | \psi_{\zeta'} \psi_{\xi'} \rangle \\ & = \sum_L \frac{4\pi}{2l+1} G(1, m_{\zeta'}; L|1, m_\zeta) G(2, m_\xi; L|2, m_{\xi'}) \\ & \quad \times F^l(2p, 3d) \delta_{\sigma_\zeta, \sigma_{\zeta'}} \delta_{\sigma_\xi, \sigma_{\xi'}}, \end{aligned} \quad (\text{A4})$$

$$\begin{aligned} & \langle \psi_\zeta \psi_\xi | v_{ee} | \psi_{\xi'} \psi_{\zeta'} \rangle \\ & = \sum_L \frac{4\pi}{2l+1} G(2, m_{\xi'}; L|1, m_\zeta) G(2, m_\xi; L|1, m_{\zeta'}) \\ & \quad \times G^l(2p, 3d) \delta_{\sigma_\zeta, \sigma_{\xi'}} \delta_{\sigma_\xi, \sigma_{\zeta'}}, \end{aligned} \quad (\text{A5})$$

where the angular momentum index L is shorthand notation for (l, m) . $F^l(2p, 3d)$ and $G^l(2p, 3d)$ are the l th order of the Slater-Condon parameters. We set $(F^0, F^2; G^1, G^3)$ to $(2, 0; 2, 0)$ in the unit of electronvolt.

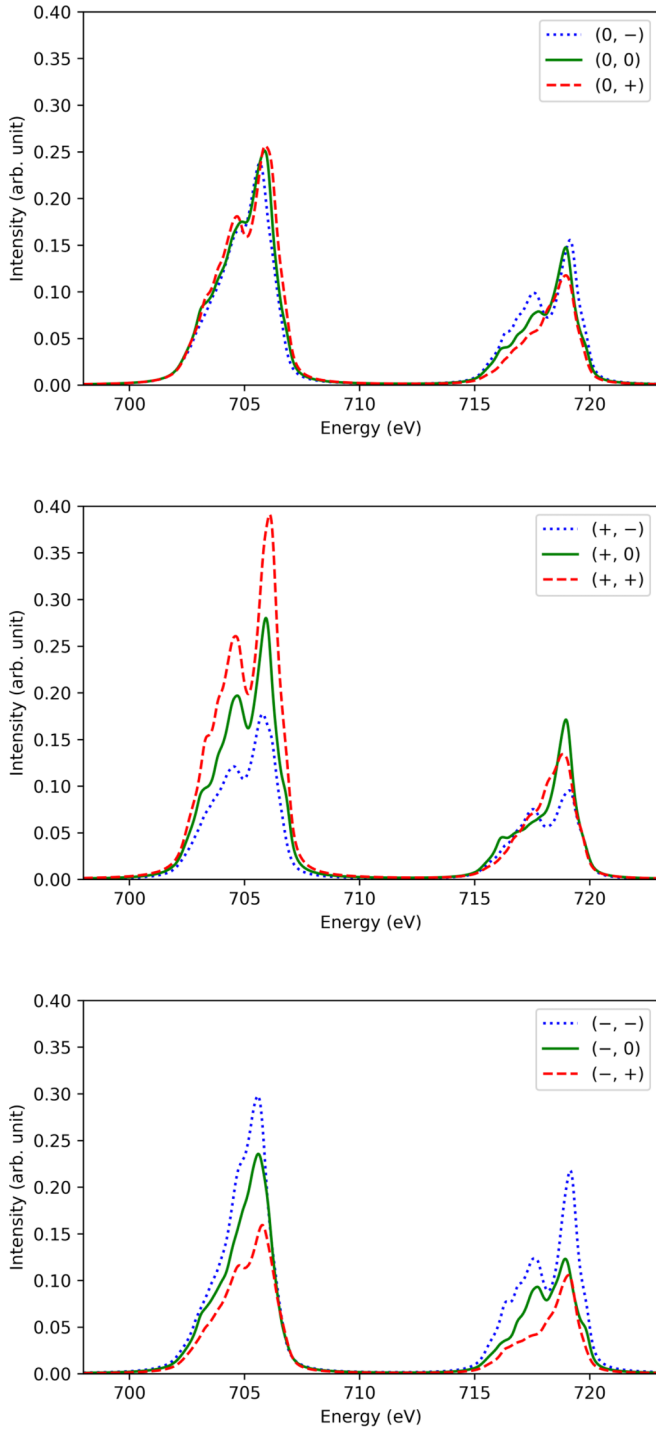


FIG. 6. Calculated L -edge XMCPE spectra for metallic iron within the Hartree-Fock approximation. The polarization of the incident and emitted photons are denoted by (λ_i, λ_f) . The emission intensity is normalized by the integral of the spectrum with the polarization of $(0, 0)$.

$G^{+,3d}$ is approximated to $\bar{G}^{+,3d}$ within the Hartree-Fock approximation:

$$-i \sum_{\mathbf{k}_d} \bar{G}_{\mathbf{k}_d \xi, \mathbf{k}_d \xi'}^{+,3d}(\omega_d) \propto \sum_{\gamma} u_{m_\xi}^\gamma u_{m_{\xi'}}^{\gamma*} \mathcal{D}_{\gamma \sigma_d}(\omega_d) f(\omega_d), \quad (\text{A6})$$

TABLE I. Integral values of spectral intensities obtained from the sum rules are compared with those calculated by DOS \mathcal{D} .

Integral/ I_n	From spectra	From DOS
I_{LS}	-0.007695	0
I_L	-0.000010	0
I_Q	3.333069	3.333269
$I_{TS}^{(1)}$	0.058986	0.054975
$I_{TS}^{(2)}$	0.213275	0.201574
I_S	-0.140879	-0.164887
I_T	0.009019	0.000009

$$\mathcal{D}_{\gamma \sigma_d}(\omega_d) = \frac{2\pi}{N} \sum_{\mathbf{k}_d} \left[-\frac{1}{\pi} \text{Im} \left(\frac{1}{\omega_d - E_{\mathbf{k}_d \gamma \sigma_d} + i\eta_D} \right) \right], \quad (\text{A7})$$

where \mathcal{D} is the density of states (DOS) in the $3d$ shell and f is the Fermi distribution function. The energy origin is chosen to the Fermi energy. η_D is a broadening parameter and its value is set to 0.01 eV as a substantially small value.

Figure 6 shows calculated L -edge XMCPE spectra by using Eq. (36) for metallic iron without the Gaussian broadening. The incident and emitted x-ray angles (β_i and β_f) are set to 0° . The detailed parameter settings are the same as those for K -edge XMCPE shown in Ref. [24]. The origin of the calculated emission energies is shifted to be consistent with the reported x-ray emission energy [30]. In Table I the values obtained by the sum rules are compared with those calculated by \mathcal{D} . The deviation of the value of I_S/I_n is about 20%, which comes from the deviation of the calculated $u_{m,\sigma}^{j,\mu}$ from the Clebsch-Gordan coefficients. It is confirmed that the deviation for I_S/I_n as well as for the other integrals becomes less than a few percentages by using the exact Clebsch-Gordan coefficients instead of the calculated $u_{m,\sigma}^{j,\mu}$.

APPENDIX B

In this Appendix, we show details of the dipole transition matrices $w^{\vec{d},2p}$ and $w^{3d,2p}$ and the derivation of Eq. (36).

We use the following relation in order to convert the velocity form to the length form of the dipole matrices:

$$[x - X, H_e] = ip_x(X), \quad (\text{B1})$$

$$p_x(X) \equiv \frac{1}{i} \frac{\partial}{\partial(x - X)}, \quad (\text{B2})$$

$$H_e |n\rangle = E_n |n\rangle, \quad (\text{B3})$$

where H_e is the electron Hamiltonian and X is a classical number and a position in the x direction. Within the dipole approximation, a transition matrix can be represented as follows [31]:

$$\begin{aligned} & \sum_i e^{i\mathbf{Q}\cdot\mathbf{R}_i} \langle n | \hat{\epsilon}_\lambda(\beta) \cdot \mathbf{p}(\mathbf{R}_i) | n' \rangle \\ & \propto \sum_i e^{i\mathbf{q}\cdot\mathbf{R}_i} (E_{n'} - E_n) \langle n | r_i Y_{1,\lambda}[\hat{r}_i(\beta)] | n' \rangle, \end{aligned} \quad (\text{B4})$$

$$\mathbf{Q} \cdot \hat{\epsilon}_\lambda(\beta) = 0, \quad (\text{B5})$$

$$\mathbf{R}_i = (X_i, Y_i, Z_i), \quad (\text{B6})$$

$$\mathbf{r}_i(\beta) = R(\beta)(\mathbf{r} - \mathbf{R}_i)R^{-1}(\beta) \equiv R(\beta)\mathbf{r}_iR^{-1}(\beta), \quad (\text{B7})$$

$$Y_{1,\lambda}[\hat{r}_i(\beta)] = \sum_{\bar{m}} Y_{1,\bar{m}}(\hat{r}_i) d_{\bar{m},\lambda}^{(1)}(\beta), \quad (\text{B8})$$

where \mathbf{Q} and \mathbf{q} are the momentum vector in the extended zone scheme and the crystal-momentum vector in the first Brillouin zone, for a photon with the polarization λ , respectively. \mathbf{R}_i is

the position vector at the lattice point i . The operator $R(\beta)$ rotates a vector at an angle β in the y axis. For the linear polarization ($\lambda = 0$) β corresponds to the angle between the polarization and magnetization directions, while for circular polarization ($\lambda = \pm 1$) β corresponds to the angle between the photon propagation and magnetization directions. $d^{(1)}$ is the orthogonal Wigner's small d matrix for the first order. In this paper, the eigenstates for the transition matrices are approximated to the Hartree-Fock solutions.

First, $w^{\bar{d},2p}$ can be calculated as follows:

$$\begin{aligned} w_{\bar{\mathbf{K}}\bar{\sigma},\mathbf{k}_p\zeta}^{\bar{d},2p}(\Lambda_i) &\propto \frac{1}{\sqrt{\varepsilon_i}} \frac{1}{\sqrt{N}} \sum_{i,i_p} e^{i\mathbf{q}_i \cdot \mathbf{R}_i} e^{i\mathbf{k}_p \cdot \mathbf{R}_{i_p}} \langle \psi_{\bar{\mathbf{K}},\bar{\sigma}}^{\bar{d}} | \hat{\varepsilon}_{\lambda_i}(\beta_i) \cdot \mathbf{p}(\mathbf{R}_i) | \psi_{i_p,\zeta}^{2p} \rangle \\ &\propto \frac{1}{\sqrt{N}} \sum_{i,i_p} e^{i\mathbf{q}_i \cdot \mathbf{R}_i} e^{i\mathbf{k}_p \cdot \mathbf{R}_{i_p}} \sum_{\bar{\zeta},j,\mu} \frac{E_{j,\mu} - \varepsilon_{\bar{K}}}{\sqrt{\varepsilon_i}} (u_{\bar{\zeta}}^{j,\mu} u_{j,\mu}^{\bar{\zeta}}) \langle \psi_{\bar{\mathbf{K}},\bar{\sigma}}^{\bar{d}} | r_i Y_{1,\lambda_i}[\hat{r}_i(\beta_i)] | \psi_{i_p,\zeta}^{2p} \rangle \\ &\approx \frac{1}{\sqrt{N}} \frac{\bar{E}_{2p} - \varepsilon_{\bar{K}}}{\sqrt{\varepsilon_i}} \sum_{i,i_p} e^{i\mathbf{q}_i \cdot \mathbf{R}_i} e^{i\mathbf{k}_p \cdot \mathbf{R}_{i_p}} \langle \psi_{\bar{\mathbf{K}},\bar{\sigma}}^{\bar{d}} | r_i Y_{1,\lambda_i}[\hat{r}_i(\beta_i)] | \psi_{i_p,\zeta}^{2p} \rangle, \end{aligned} \quad (\text{B9})$$

where \bar{E}_{2p} is the average value of the eigenvalues of \bar{H}_{2p} . The wave functions $\psi^{\bar{d}}$ and ψ^{2p} are defined by

$$\langle \mathbf{r} | \psi_{\bar{\mathbf{K}},\bar{\sigma}}^{\bar{d}} \rangle = \frac{1}{\sqrt{\Omega}} e^{i\bar{\mathbf{K}} \cdot \mathbf{r}} |\bar{\sigma}\rangle, \quad \langle \mathbf{r} | \psi_{i_p,\zeta}^{2p} \rangle = \psi_{2p}(r_{i_p}) Y_{1,m_\zeta}(\hat{r}_{i_p}) |\sigma_\zeta\rangle, \quad (\text{B10})$$

where Ω is the volume of a unit cell. Bauer's formula is useful to calculate a plane wave function:

$$e^{i\mathbf{K} \cdot \mathbf{r}} = 4\pi \sum_L i^l j_l(Kr) Y_L(\hat{r}) Y_L^*(\hat{\mathbf{K}}), \quad (\text{B11})$$

where j_l is the spherical Bessel function for the order l . The bracket part in Eq. (B9) is approximated as follows:

$$\langle \psi_{\bar{\mathbf{K}},\bar{\sigma}}^{\bar{d}} | r_i Y_{1,\lambda_i}[\hat{r}_i(\beta_i)] | \psi_{i_p,\zeta}^{2p} \rangle = \frac{\delta_{\bar{\sigma},\sigma_\zeta}}{\sqrt{\Omega}} \int d\mathbf{r} e^{-i\bar{\mathbf{K}} \cdot \mathbf{r}} r_i Y_{1,\lambda_i}[\hat{r}_i(\beta_i)] \psi_{2p}(r_{i_p}) Y_{1,m_\zeta}(\hat{r}_{i_p}) \approx \frac{\delta_{\bar{\sigma},\sigma_\zeta}}{\sqrt{\Omega}} e^{-i\bar{\mathbf{K}} \cdot \mathbf{R}_{i_p}} I_{m_\zeta,\lambda_i}(\bar{\mathbf{K}}; \beta_i) \delta_{i,i_p}, \quad (\text{B12})$$

$$I_{m_\zeta,\lambda_i}(\bar{\mathbf{K}}; \beta_i) = 4\pi i^2 I_2(\bar{K}) \sum_{m,m'} G(1m_\zeta, 1m'|2m) d_{m',\lambda_i}^{(1)}(\beta_i) Y_{2,m}(-\hat{\bar{K}}) + 4\pi i^0 I_0(\bar{K}) \sum_{m'} G(1m_\zeta, 1m'|00) d_{m',\lambda_i}^{(1)}(\beta_i) Y_{00}, \quad (\text{B13})$$

$$I_l(\bar{K}) = \int dr r^3 j_l(\bar{K}r) \psi_{2p}(r). \quad (\text{B14})$$

Therefore,

$$w_{\bar{\mathbf{K}}\bar{\sigma},\mathbf{k}_p\zeta}^{\bar{d},2p}(\Lambda_i) \propto \frac{1}{\sqrt{N}} \frac{\bar{E}_{2p} - \varepsilon_{\bar{K}}}{\sqrt{\varepsilon_i}} \delta_{\bar{\sigma},\sigma_\zeta} I_{m_\zeta,\lambda_i}(\bar{\mathbf{K}}; \beta_i) \sum_{i_p} e^{i(\mathbf{k}_p + \mathbf{q}_i - \bar{\mathbf{k}}) \cdot \mathbf{R}_{i_p}} = \delta_{\mathbf{k}_p + \mathbf{q}_i, \bar{\mathbf{k}}} \delta_{\bar{\sigma},\sigma_\zeta} \sqrt{N} \frac{\bar{E}_{2p} - \varepsilon_{\bar{K}}}{\sqrt{\varepsilon_i}} I_{m_\zeta,\lambda_i}(\bar{\mathbf{K}}; \beta_i), \quad (\text{B15})$$

$$(w_{\bar{\mathbf{K}}\bar{\sigma},\bar{\mathbf{k}}_p\bar{\zeta}}^{\bar{d},2p}(\Lambda_i))^* w_{\bar{\mathbf{K}}\bar{\sigma},\mathbf{k}_p\zeta}^{\bar{d},2p}(\Lambda_i) \approx \delta_{\bar{\mathbf{k}}_p + \mathbf{q}_i, \bar{\mathbf{k}}} \delta_{\mathbf{k}_p + \mathbf{q}_i, \bar{\mathbf{k}}} \delta_{\bar{\sigma},\sigma_\zeta} \delta_{\bar{\sigma},\sigma_\zeta} N \left(\frac{\bar{E}_{2p} - \varepsilon_{\bar{K}}}{\sqrt{\varepsilon_i}} \right)^2 I_{m_{\zeta'},\lambda_i}^*(\bar{\mathbf{K}}; \beta_i) I_{m_\zeta,\lambda_i}(\bar{\mathbf{K}}; \beta_i). \quad (\text{B16})$$

If \bar{K} is large enough to satisfy $\bar{G} \gg \bar{k}$, then we can use

$$\sum_{\bar{\mathbf{K}}} f(\bar{\mathbf{K}}) \approx \sum_{\bar{\mathbf{G}}} f(\bar{\mathbf{G}}) \propto \sum_{\bar{\mathbf{k}}} \int d\bar{\mathbf{G}} f(\bar{\mathbf{G}}), \quad (\text{B17})$$

where f is any function of $\bar{\mathbf{K}}$. This approximation allows the solid-angle integration of $I_{m_{\zeta'},\lambda_i}^* I_{m_\zeta,\lambda_i}$, which eliminates the off-diagonal terms:

$$\begin{aligned} \int d\bar{\mathbf{G}} I_{m_{\zeta'},\lambda_i}^*(\bar{\mathbf{G}}; \beta_i) I_{m_\zeta,\lambda_i}(\bar{\mathbf{G}}; \beta_i) &\propto (I_2(\bar{G}))^2 M_{m_{\zeta'},m_\zeta;\lambda_i}^{\bar{d},2p}(\beta_i; R_{02}), \\ M_{m_{\zeta'},m_\zeta;\lambda_i}^{\bar{d},2p}(\beta_i; R_{02}) &\equiv \sum_{\bar{m}} G(1, m_{\zeta'}; 1, \bar{m} - m_{\zeta'} | 2, \bar{m}) d_{\bar{m}-m_{\zeta'},\lambda_i}^{(1)}(\beta_i) G(1, m_\zeta; 1, \bar{m} - m_\zeta | 2, \bar{m}) d_{\bar{m}-m_\zeta,\lambda_i}^{(1)}(\beta_i) \\ &\quad + R_{02} d_{-m_{\zeta'},\lambda_i}^{(1)}(\beta_i) d_{-m_\zeta,\lambda_i}^{(1)}(\beta_i), \end{aligned} \quad (\text{B18})$$

where R_{02} is originally $(I_0(\tilde{G})/I_2(\tilde{G}))^2$ but treated as a parameter in this paper. In order to obtain sum rules, R_{02} is set to 0 and $M^{\tilde{d},2p}(\beta_i) \equiv M^{\tilde{d},2p}(\beta_i; 0)$. The following relation is useful to derive Eq. (36):

$$\begin{aligned} \sum_{\tilde{\mathbf{G}}} (w_{\tilde{\mathbf{k}}\tilde{\sigma},\tilde{\mathbf{k}}_p\tilde{\zeta}'}^{\tilde{d},2p}(\Lambda_i))^* w_{\tilde{\mathbf{k}}\tilde{\sigma},\mathbf{k}_p\zeta}^{\tilde{d},2p}(\Lambda_i) f(\tilde{\mathbf{K}}) &\approx N \delta_{\tilde{\mathbf{k}},\tilde{\mathbf{k}}_p+\mathbf{q}_i} \delta_{\tilde{\mathbf{k}},\mathbf{k}_p+\mathbf{q}_i} \delta_{\tilde{\sigma},\sigma_{\zeta'}} \delta_{\tilde{\sigma},\sigma_{\zeta}} M_{m_{\zeta'},m_{\zeta};\lambda_i}^{\tilde{d},2p}(\beta_i) \int d\tilde{G} \tilde{G}^2 I^{\tilde{d},2p}(\tilde{G}, \varepsilon_i) f(\tilde{G}) \\ &\propto N \delta_{\tilde{\mathbf{k}},\tilde{\mathbf{k}}_p+\mathbf{q}_i} \delta_{\tilde{\mathbf{k}},\mathbf{k}_p+\mathbf{q}_i} \delta_{\tilde{\sigma},\sigma_{\zeta'}} \delta_{\tilde{\sigma},\sigma_{\zeta}} M_{m_{\zeta'},m_{\zeta};\lambda_i}^{\tilde{d},2p}(\beta_i) \int d\varepsilon \rho_0(\varepsilon) I^{\tilde{d},2p}(\tilde{G}_\varepsilon, \varepsilon_i) f(\tilde{G}_\varepsilon), \end{aligned} \quad (\text{B19})$$

$$\tilde{G}_\varepsilon = \sqrt{2\varepsilon}, \quad (\text{B20})$$

$$I^{\tilde{d},2p}(\tilde{G}_\varepsilon, \varepsilon_i) = \left(\frac{\bar{E}_{2p} - \varepsilon}{\sqrt{\varepsilon_i}} \right)^2 (I_2(\tilde{G}_\varepsilon))^2, \quad (\text{B21})$$

where ρ_0 is the free electron density of states.

By using Eq. (B19), the terms related to $\tilde{\mathbf{K}}$ in Eq. (33) are simplified as follows:

$$\begin{aligned} \sum_{\tilde{\mathbf{K}}} (w_{\tilde{\mathbf{k}}\tilde{\sigma},\tilde{\mathbf{k}}_p\tilde{\zeta}'}^{\tilde{d},2p}(\Lambda_i))^* w_{\tilde{\mathbf{k}}\tilde{\sigma},\mathbf{k}_p\zeta}^{\tilde{d},2p}(\Lambda_i) \delta(\varepsilon_{\tilde{\mathbf{K}}} - \varepsilon_{if}(\omega_d)) \\ \approx N \delta_{\tilde{\mathbf{k}},\mathbf{k}_p+\mathbf{q}_i} \delta_{\tilde{\mathbf{k}},\tilde{\mathbf{k}}_p+\mathbf{q}_i} \delta_{\tilde{\sigma},\sigma_{\zeta'}} \delta_{\tilde{\sigma},\sigma_{\zeta}} M_{m_{\zeta'},m_{\zeta};\lambda_i}^{\tilde{d},2p}(\beta_i) \int d\varepsilon \rho_0(\varepsilon) I^{\tilde{d},2p}(\tilde{G}_\varepsilon, \varepsilon_i) \delta(\varepsilon - \varepsilon_{if}(\omega_d)) \\ = N \delta_{\tilde{\mathbf{k}},\mathbf{k}_p+\mathbf{q}_i} \delta_{\tilde{\mathbf{k}},\tilde{\mathbf{k}}_p+\mathbf{q}_i} \delta_{\tilde{\sigma},\sigma_{\zeta'}} \delta_{\tilde{\sigma},\sigma_{\zeta}} M_{m_{\zeta'},m_{\zeta};\lambda_i}^{\tilde{d},2p}(\beta_i) \rho_0(\varepsilon_{if}(\omega_d)) I^{\tilde{d},2p}(\tilde{G}_{\varepsilon_{if}(\omega_d)}, \varepsilon_i). \end{aligned} \quad (\text{B22})$$

The order of $\varepsilon_{if}(\omega_d)$ is dominated by that of $(\varepsilon_i - \varepsilon_f)$, which is assumed to be a few kiloelectronvolts. Thus $\delta(\varepsilon_{\tilde{\mathbf{K}}} - \varepsilon_{if}(\omega_d))$ restricts the order of $\varepsilon_{\tilde{\mathbf{K}}}$ to a few kiloelectronvolts, which ensures $\tilde{G} \gg \tilde{k}$ and justifies using Eqs. (B17) and (B19). Because the order of the energy range of ω_d is tens of electronvolts and substantially smaller than the order of $(\varepsilon_i - \varepsilon_f)$, the ω_d dependence of ε_{if} can be neglected. In addition, the order of $\Delta\varepsilon_f[\equiv |\max(\varepsilon_f) - \min(\varepsilon_f)|]$ is the same as $\Delta\omega_d[\equiv |\max(\omega_d) - \min(\omega_d)|]$. These energy-order estimations approximate ρ_0 and $I^{\tilde{d},2p}$ to constants (recall that ε_i is fixed and treated as a constant).

Next, $w_{\mathbf{k}_d\xi,\mathbf{k}_p\zeta}^{3d,2p}$ can be calculated as follows:

$$\begin{aligned} w_{\mathbf{k}_d\xi,\mathbf{k}_p\zeta}^{3d,2p}(\Lambda_f) &\propto \frac{1}{\sqrt{\varepsilon_f}} \frac{1}{N} \sum_{i_d,i_f,i_p} e^{-i\mathbf{k}_d \cdot \mathbf{R}_{i_d}} e^{i\mathbf{q}_f \cdot \mathbf{R}_{i_f}} e^{i\mathbf{k}_p \cdot \mathbf{R}_{i_p}} \langle \psi_{i_d,\xi}^{3d} | \hat{\varepsilon}_{\lambda_f}(\beta_f) \cdot \mathbf{p}_{i_f} | \psi_{i_p,\zeta}^{2p} \rangle \\ &\propto \frac{1}{\sqrt{\varepsilon_f}} \frac{1}{N} \sum_{i_d,i_f,i_p} e^{-i\mathbf{k}_d \cdot \mathbf{R}_{i_d}} e^{i\mathbf{q}_f \cdot \mathbf{R}_{i_f}} e^{i\mathbf{k}_p \cdot \mathbf{R}_{i_p}} \sum_{\xi,\gamma} \sum_{\bar{\zeta},j,\mu} \frac{E_{j,\mu} - \varepsilon_\gamma(\mathbf{k}_d)}{\sqrt{\varepsilon_f}} (u_\xi^\gamma u_{\bar{\zeta}}^\gamma)^* (u_\xi^{j,\mu} u_{j,\mu}^{\bar{\zeta}}) \langle \psi_{i_d,\xi}^{3d} | r_{i_f} Y_{1,\lambda_f}[\hat{r}_{i_f}(\beta_f)] | \psi_{i_p,\bar{\zeta}}^{2p} \rangle \\ &\approx \frac{1}{\sqrt{\varepsilon_f}} \frac{1}{N} \frac{\bar{E}_{2p} - \bar{\varepsilon}_{3d}}{\sqrt{\varepsilon_f}} \sum_{i_d,i_f,i_p} e^{-i\mathbf{k}_d \cdot \mathbf{R}_{i_d}} e^{i\mathbf{q}_f \cdot \mathbf{R}_{i_f}} e^{i\mathbf{k}_p \cdot \mathbf{R}_{i_p}} \langle \psi_{i_d,\xi}^{3d} | r_{i_f} Y_{1,\lambda_f}[\hat{r}_{i_f}(\beta_f)] | \psi_{i_p,\zeta}^{2p} \rangle, \end{aligned} \quad (\text{B23})$$

where $\bar{\varepsilon}_{3d}$ is the average of the eigenvalues of H_{band} . The bracket part is approximated as follows:

$$\langle \psi_{i_d,\xi}^{3d} | r_{i_p} Y_{1,\lambda_f}[\hat{r}_{i_p}(\beta_f)] | \psi_{i_p,\zeta}^{2p} \rangle \approx \delta_{\sigma_\xi,\sigma_\zeta} \delta_{i_d,i_f} \delta_{i_f,i_p} \langle \psi_{i_f,\xi}^{3d} | r_{i_f} Y_{1,\lambda_f}[\hat{r}_{i_f}(\beta_f)] | \psi_{i_f,\zeta}^{2p} \rangle, \quad (\text{B24})$$

$$\langle \psi_{i_f,\xi}^{3d} | r_{i_f} Y_{1,\lambda_f}[\hat{r}_{i_f}(\beta_f)] | \psi_{i_f,\zeta}^{2p} \rangle = \left(\int dr_i r_i^3 \psi_{3d,\xi}(r_i) \psi_{2p}(r_i) \right) \left(\int d\hat{r}_i Y_{2,m_\xi}^*(\hat{r}_i) Y_{1,\lambda_f}[\hat{r}_i(\beta_f)] Y_{1,m_\zeta}(\hat{r}_i) \right) \equiv I_\xi M_{m_\xi,m_\zeta;\lambda_f}^{3d,2p}(\beta_f), \quad (\text{B25})$$

$$I_\xi = \int dr r^3 \psi_{3d,\xi}(r) \psi_{2p}(r), \quad (\text{B26})$$

$$M_{m_\xi,m_\zeta;\lambda_f}^{3d,2p}(\beta_f) = G(1, m_\zeta; 1, m_\xi - m_\zeta | 2, m_\xi) d_{m_\xi - m_\zeta, \lambda_f}^{(1)}(\beta_f). \quad (\text{B27})$$

Therefore,

$$\begin{aligned} w_{\mathbf{k}_d\xi,\mathbf{k}_p\zeta}^{3d,2p}(\Lambda_f) &\approx \delta_{\mathbf{k}_d,\mathbf{k}_p+\mathbf{q}_f} \delta_{\sigma_\xi,\sigma_\zeta} \frac{\bar{E}_{2p} - \bar{\varepsilon}_{3d}}{\sqrt{\varepsilon_f}} I_\xi M_{m_\xi,m_\zeta;\lambda_f}^{3d,2p}(\beta_f) \\ &\equiv \delta_{\mathbf{k}_d,\mathbf{k}_p+\mathbf{q}_f} \delta_{\sigma_\xi,\sigma_\zeta} I_\xi^{3d,2p}(\varepsilon_f) M_{m_\xi,m_\zeta;\lambda_f}^{3d,2p}(\beta_f), \end{aligned} \quad (\text{B28})$$

$$I_\xi^{3d,2p}(\varepsilon_f) = \frac{\bar{E}_{2p} - \bar{\varepsilon}_{3d}}{\sqrt{\varepsilon_f}} I_\xi. \quad (\text{B29})$$

In order to derive sum rules, we assume the m -independent radial $3d$ wave functions ($\psi_{3d,\xi} \approx \psi_{3d}$), which makes $I_{\xi}^{3d,2p} \approx I^{3d,2p}$. Because $\Delta\varepsilon_f$ is substantially smaller than the order of $(\bar{E}_{2p} - \bar{\varepsilon}_{3d})^2$, the ε_f dependence of $I^{3d,2p}$ can be neglected, which approximates $I^{3d,2p}$ to a constant.

Finally, combining Eqs. (33), (B22), and (B28) leads to Eq. (36).

APPENDIX C

In this Appendix, we show that the representation of the characteristic function $\chi_{m'}(m)$ is determined uniquely in $(\beta_i, \beta_f) = (0, 0)$. The eigenvectors \mathbf{e}^m of L_z are defined by

$$\mathbf{e}^m = (0, \dots, 0, 1, 0, \dots, 0)^T \in \mathbb{R}^5, \quad (\text{C1})$$

where \mathbf{e}^m has the unit value only for the m component. By the definition of \mathbf{e}^m , the components of \mathbf{e}^m work like the Kronecker delta:

$$(\mathbf{e}^{m'})_m = \delta_{m',m}. \quad (\text{C2})$$

In order to construct a basis of \mathbb{R}^5 , we define the following vector:

$$\mathbf{V}_{L_z}^n \equiv (2^n \quad 1^n \quad 0^n \quad (-1)^n \quad (-2)^n)^T, \quad (\text{C3})$$

$$(\mathbf{V}_{L_z}^n)_m = m^n, \quad (\text{C4})$$

where $0^0 \equiv 1$ in order to define $\mathbf{V}_{L_z}^0$ as the vector all of whose elements are one. $\mathbf{V}_{L_z}^n$ corresponds to the vector extracting only the diagonal components in the matrix form of $(L_z)^n$ represented by its eigenvectors with $l = 2$.

It can be shown that $\mathbf{V}_{L_z}^n$ ($n = 0, \dots, 4$) is a basis of \mathbb{R}^5 as follows:

$$B \equiv (\mathbf{V}_{L_z}^0, \mathbf{V}_{L_z}^1, \mathbf{V}_{L_z}^2, \mathbf{V}_{L_z}^3, \mathbf{V}_{L_z}^4), \quad (\text{C5})$$

$$\det(B) \neq 0. \quad (\text{C6})$$

Thus \mathbf{e}^m can be obtained by the linear combination of $\mathbf{V}_{L_z}^n$:

$$\mathbf{e}^m \equiv B^{-1} \mathbf{e}^m, \quad (\text{C7})$$

$$(\mathbf{B}\mathbf{e}^{m'})_m = \sum_{n=0}^4 (\mathbf{e}^{m'})_n m^n = \delta_{m',m}. \quad (\text{C8})$$

Therefore, $\chi_{m'}(m)$ can be obtained by

$$\chi_{m'}(m) \equiv \sum_{n=0}^4 (\mathbf{e}^{m'})_n m^n. \quad (\text{C9})$$

Because $\chi_{m'}(m)$ is a polynomial of m ($= 0, \pm 1, \pm 2$), any function of m can be expressed by a polynomial of m . For an example of $F(m) = f_0 \delta_{m,0}$ and $G(m) = g_1 \delta_{m,1}$, when m is restricted to $m = 0, \pm 1, \pm 2$, the Kronecker delta can be replaced by the characteristic function. As a result, $F(m) + G(m)$ can be represented by

$$F(m) + G(m) = \left(\frac{f_0}{4} - \frac{g_1}{6}\right)m^4 - \frac{g_1}{6}m^3 + \left(-\frac{5}{4}f_0 + \frac{4}{6}g_1\right)m^2 + \frac{4}{6}g_1 m + f_0. \quad (\text{C10})$$

Thus, unlike the Kronecker delta, the characteristic function allows one to perform calculations flexibly.

-
- | | |
|--|---|
| <p>[1] G. Schütz, W. Wagner, W. Wilhelm, P. Kienle, R. Zeller, R. Frahm, and G. Materlik, <i>Phys. Rev. Lett.</i> 58, 737 (1987).</p> <p>[2] J. Stöhr and H. C. Siegmann, <i>Magnetism from Fundamentals to Nanoscale Dynamics</i> (Springer-Verlag, Berlin, 2006).</p> <p>[3] <i>Magnetism: A Synchrotron Radiation Approach</i>, edited by E. Beaurepaire, H. Bulou, F. Scheurer, and J. P. Kappler (Springer-Verlag, Berlin, 2006).</p> <p>[4] B. T. Thole, P. Carra, F. Sette, and G. van der Laan, <i>Phys. Rev. Lett.</i> 68, 1943 (1992).</p> | <p>[5] P. Carra, B. T. Thole, M. Altarelli, and X. Wang, <i>Phys. Rev. Lett.</i> 70, 694 (1993).</p> <p>[6] M. Altarelli, <i>Phys. Rev. B</i> 47, 597 (1993).</p> <p>[7] A. Ankudinov and J. J. Rehr, <i>Phys. Rev. B</i> 51, 1282 (1995).</p> <p>[8] C. T. Chen, Y. U. Idzerda, H.-J. Lin, N. V. Smith, G. Meigs, E. Chaban, G. H. Ho, E. Pellegrin, and F. Sette, <i>Phys. Rev. Lett.</i> 75, 152 (1995).</p> <p>[9] G. Y. Guo, <i>J. Phys.: Condens. Matter</i> 8, L747 (1996).</p> |
|--|---|

- [10] J. Kogo, K. Niki, and T. Fujikawa, *J. Phys. Soc. Jpn.* **89**, 064709 (2020).
- [11] P. Strange, P. J. Durham, and B. L. Gyorffy, *Phys. Rev. Lett.* **67**, 3590 (1991).
- [12] C. F. Hague, J.-M. Mariot, P. Strange, P. J. Durham, and B. L. Gyorffy, *Phys. Rev. B* **48**, 3560 (1993).
- [13] M. H. Krisch, F. Sette, U. Bergmann, C. Masciovecchio, R. Verbeni, J. Goulon, W. Caliebe, and C. C. Kao, *Phys. Rev. B* **54**, R12673 (1996).
- [14] F. M. F. de Groot, M. Nakazawa, A. Kotani, M. H. Krisch, and F. Sette, *Phys. Rev. B* **56**, 7285 (1997).
- [15] L.-C. Duda, J. Stöhr, D. C. Mancini, A. Nilsson, N. Wassdahl, J. Nordgren, and M. G. Samant, *Phys. Rev. B* **50**, 16758 (1994).
- [16] C.-F. Hague, J.-M. Mariot, G. Y. Guo, K. Hricovini, and G. Krill, *Phys. Rev. B* **51**, 1370 (1995).
- [17] T. Iwazumi, K. Kobayashi, S. Kishimoto, T. Nakamura, S. Nanao, D. Ohsawa, R. Katano, and Y. Isozumi, *Phys. Rev. B* **56**, R14267 (1997).
- [18] L. Braicovich, G. van der Laan, G. Ghiringhelli, A. Tagliaferri, M. A. van Veenendaal, N. B. Brookes, M. M. Chervinskii, C. Dallera, B. DeMichelis, and H. A. Dürr, *Phys. Rev. Lett.* **82**, 1566 (1999).
- [19] M. Sikora, A. Juhin, T.-C. Weng, P. Sainctavit, C. Detlefs, F. de Groot, and P. Glatzel, *Phys. Rev. Lett.* **105**, 037202 (2010).
- [20] M. Sikora, A. Juhin, G. Simon, M. Zajac, K. Biernacka, C. Kapusta, L. Murellon, M. R. Ibarra, and P. Glatzel, *J. Appl. Phys.* **111**, 07E301 (2012).
- [21] J. Miyawaki, S. Suga, H. Fujiwara, M. Urasaki, H. Ikeno, H. Niwa, H. Kiuchi, and Y. Harada, *Phys. Rev. B* **96**, 214420 (2017).
- [22] P. Zimmermann, N. Bouildi, M. O. J. Y. Hunault, M. Sikora, J. M. Ablett, J.-P. Rueff, B. Lebert, P. Sainctavit, F. M. F. de Groot, and A. Juhin, *J. Electron Spectrosc. Relat. Phenom.* **222**, 74 (2018).
- [23] T. Inami, *Phys. Rev. Lett.* **119**, 137203 (2017).
- [24] A. Koide, T. Nomura, and T. Inami, *Phys. Rev. B* **102**, 224425 (2020).
- [25] P. Nozières and E. Abrahams, *Phys. Rev. B* **10**, 3099 (1974).
- [26] L. V. Keldysh, *J. Exptl. Theoret. Phys. (U.S.S.R.)* **47**, 1515 (1964) [*Sov. Phys. JETP* **20**, 1018 (1965)].
- [27] See Supplemental Material at <http://link.aps.org/supplemental/10.1103/PhysRevB.104.094419> for the dependence of the integral of L -edge XMCPE spectra on the incident and emitted x-ray angles.
- [28] K. Hirano, K. Izumi, T. Ishikawa, S. Annaka, and S. Kikuta, *Jpn. J. Appl. Phys., Part 2* **30**, L407 (1991).
- [29] J. P. Perdew, K. Burke, and M. Ernzerhof, *Phys. Rev. Lett.* **77**, 3865 (1996).
- [30] M. Terauchi, H. Takahashi, M. Takakura, T. Murano, and S. Koshiya, *Handbook of Soft X-ray Emission Spectra Version 6.0* (Sep. 2020), https://www.jeol.co.jp/en/download_soft_x-ray.html
- [31] L. J. P. Ament, M. van Veenendaal, T. P. Devereaux, J. P. Hill, and J. van den Brink, *Rev. Mod. Phys.* **83**, 705 (2011).